ELSEVIER

Contents lists available at ScienceDirect

International Journal of Mechanical Sciences

journal homepage: www.elsevier.com/locate/ijmecsci



Fractional-order structural stability: Formulation and application to the critical load of nonlocal slender structures



Sai Sidhardh, Sansit Patnaik, Fabio Semperlotti*

School of Mechanical Engineering, Ray W. Herrick Laboratories, Purdue University, West Lafayette, IN 47907, USA

ARTICLE INFO

Keywords: Fractional calculus Nonlocal elasticity Stability Energy methods Critical buckling load

ABSTRACT

This study presents a framework to perform stability analysis of nonlocal solids whose behavior is described according to the fractional-order continuum theory. In this formulation, space fractional-order operators are used to capture the nonlocal response of the medium by means of nonlocal kinematic relations. We use the geometrically nonlinear fractional-order kinematic relations within an energy based approach to establish the Lagrange-Dirichlet stability criteria for nonlocal structures. This energy based approach to nonlocal structural stability is possible due to a positive-definite and thermodynamically consistent definition of the deformation energy enabled by the fractional-order kinematic formulation. The Rayleigh-Ritz coefficient for critical load is also derived for linear buckling conditions. The fractional-order formulation is finally used to determine critical loads for buckling of the slender nonlocal beams and plates using a dedicated fractional-order finite element solver. Results establish that, in contrast to existing studies, the effect of nonlocal interactions is observed on both the material and the geometric stiffness, when using the fractional-order kinematics approach. These observations are supported quantitatively via the solution of case studies that focus on the critical buckling response of fractional-order nonlocal slender structures, and a direct comparison of the fractional-order approach with classical nonlocal approaches.

1. Introduction

The stability analysis of structures, particularly the estimation of the critical load for buckling, is a canonical problem in structural analysis and design. An extensive body of literature is available on this topic in the general area of classical (local) elasticity, which is built upon a point-wise correspondence of the kinematic and material variables via the constitutive relations. Comprehensive reviews of the stability of elastic structures following classical elasticity theories can be found in [1,2]. While this class of so-called local approaches has been, and still is, a fundamental tool to model the behavior of solids, experimental observations have shown that the nonlocal interactions between extended areas of the solid (i.e. between distant points) can have a nonnegligible effect on the global response of the medium. These effects, which are a macroscopic manifestation of long-distance interactions between distant points, are not accounted for in classical local theories. Although nonlocal effects have been traditionally restricted to the context of micro- and nano-scale systems [3,4], examples can be found in a broader range of applications including macro-scale complex media such as sandwich structures, architected materials, as well as functionally graded and porous materials [5-8].

During the past several decades, numerous theories have been proposed to model the effect of the nonlocal interactions in elastic solids. Prominent theories were proposed by Kroner [9] and Eringen et al. [10] involving strain-based integral constitutive relations. These approaches accounted for the nonlocal interactions within the constitutive relations via a convolution of the local strain with a kernel defined over the domain of influence. Other approaches include displacement based models implementing a superposition of both local and nonlocal interactions [11]. In the context of stability analysis, the critical load for buckling of the slender structures performed using the strain-based integral formulation [12,13] predicted a consistent reduction of the critical loads due to the nonlocal effect. While these strain-based integral formulations were powerful and somewhat very intuitive, the integral definition of the constitutive relation [10] belongs to an ill-posed class of integral equations involving Fredholm integral equations of the first kind, which do not admit unique solutions. Successively, gradient based models of nonlocal elasticity were developed in order to circumvent the issues typical of implicit integral formulations [14]. In most cases, the differential equivalent of the single-phase model [13,15,16] predicted a consistent reduction of the critical loads caused by the nonlocal effect, however paradoxical observations were noted for certain choices of loading and boundary conditions. These observations could be attributed to the non-self adjoint nature of the linear operators obtained following the differential models for Eringen's nonlocal elasticity [17,18]. Also, note that the differential models are equivalent to their

^{*} Corresponding author.

E-mail address: fsemperl@purdue.edu (F. Semperlotti).

integral counterparts only for certain choices of the kernel used in the convolution integral and assuming an unbounded medium [19]. To address this important issue a two-phase definition (i.e. local/non-local) of the constitutive relations was proposed. This definition admits unique solutions and is generally well-posed in nature leading to self-adjoint linear operators [20]. The critical load analysis performed using this two-phase formulation [21] also predicted a consistent reduction of the critical loads caused by the nonlocal effects. While the two-phase models present unique solutions with a consistent nonlocal nature across loading and boundary conditions, this characteristic property is lost for certain choices of the constitutive parameters. As pointed in [18,20], the inherent ill-posedness of the strain-based integral theories of nonlocal elasticity resurfaces for vanishing values of the local fraction within the two-phase nonlocal theory. This places an ad-hoc restriction on the ratio between the local and nonlocal components. Further, these strain-driven integral models also do not satisfy the thermodynamic balance laws in a rigorous manner. More specifically, it has been observed that thermomechanical deformation, obtained via this approach, satisfies the second law of thermodynamics only in a weak (integral) sense and not in a strong (localized) manner [20,22,23]. The above observations highlight that there are still some important limitations in the existing nonlocal elasticity theories that affects, although are not limited to, the stability analysis of nonlocal structures.

Recall that, in classical elasticity, the critical load is expressed as the ratio of the material and geometric stiffness associated with the structure (Rayleigh-Ritz coefficient) [1]. In the presence of long-range interactions within a nonlocal solid, it is expected that the nonlocal effects will be realized upon both of these stiffness terms. However, studies employing the Eringen's strain-integral models of nonlocal elasticity attributed the consistent decrease in the critical load to a reduction of material stiffness caused by nonlocal effects, while the geometric stiffness was essentially unaffected [12,13]. In contrast, the decrease in critical loads predicted by differential models (for those cases not leading to paradoxical observations) was attributed to an increase in geometric stiffness of the structure while the material stiffness was left unaffected [13,15]. A comparison of these contrasting approaches for the calculation of the critical load of nonlocal structures indicates that the strain-integral model predicts a sharper reduction over its equivalent differential model [24]. Following the above discussion, it is clear that both the strain-based integral and differential approaches modify either the material or the geometric stiffness [24]. However, the physical realization of the nonlocal effects should not be limited to either one of these structural stiffness terms. Clearly there is a gap in proper accounting for the nonlocal effects on the structural stiffness terms, and a clear understanding of this would be required for the stability studies of nonlocal structures.

Recently, the development of fractional-order continuum theories for nonlocal elasticity has offered alternative methodologies that could potentially help filling this gap [6,11,25]. In recent years, fractional calculus has garnered increasing attention thanks to its many applications in diverse domains of science and engineering. Successful applications in mechanics include, to name a few, constitutive modeling of viscoelastic materials to study memory effects [26-28], nonlocal effects across multiple spatial scales [25,29], dissipation in heat transfer [30]. Numerous models for nonlocal elasticity based on fractional calculus have also been proposed [6,11,25,31]. Fractional-order continuum theories have successfully modeled both softening [32,33] and stiffening [29,34] effects associated with long-range nonlocal interactions in solids, and in complex fluids [8]. Among the aforementioned literature, studies based on fractional-order kinematic approaches are particularly exciting since they have been able to address key limitations of both integral and gradient based approaches to nonlocal elasticity [6,29]. More specifically, modeling nonlocal interactions at the level of the kinematics in a frame-invariant and dimensionally consistent manner, allows obtaining localized material constitutive relations free from nonlocal residual terms. The resulting nonlocal models allowed the rigorous application of the thermodynamic principles without any physical inconsistency. In other terms, the fractional-order kinematic approach allows for a strong (or localized) imposition of the first and second laws of thermodynamics at each point within the continuum [23]. This result is unlike the classical nonlocal approaches based on the integral-form of the material constitutive relations that, instead, allow only a weak imposition of the thermodynamic balance laws over the entire domain. Further, the positive-definite deformation energy density achieved with this definition guarantees the uniqueness of the solution and allows variational principles to be applied for fractional-order continuum theories. This facilitates the development of finite element based solutions for fractionalorder models of nonlocal solids [32,33]. By means of this numerical tool, the effects of long-range interactions modeled using the fractional-order continuum theory have been studied on both the linear and the geometrically nonlinear response of nonlocal beams and plates [32,33,35,36]. Large deformation analysis of nonlocal structures can be effectively carried out using geometrically nonlinear fractional-order kinematic relations [33,36]. This framework facilitated by the fractional-order models provides the foundation required for an energy-based stability analysis of nonlocal structures. So we may conclude that the fractional-order formulation provides physically, thermodynamically, and mathematically consistent models for the softening influence of nonlocal interactions[23,32].

Before proceeding further, we provide a comparison of the fractional-order theories with other existing nonlocal models. The fractional-order continuum theory for nonlocal solids belongs to a class of displacement-driven nonlocal models, where differ-integral operators replace the classical integer-order derivatives within the straindisplacement relations. This modification follows from a fractionalorder definition of the deformation gradient tensor, and allows the constitutive models to capture long-range interactions within the nonlocal solid. The Eringen's integral theory of nonlocal elasticity [19] is based on a strain-driven approach to nonlocal elasticity. It is established that, unlike the fractional-order theory, Eringen's model does not satisfy the thermodynamic balance laws in a rigorous manner [20,37]. The thermodynamic consistency is crucial to develop well-posed governing equations. This issue with the Eringen model is inherent in all the theories derived from it such as the two-phase (local/non-local) theory of elasticity [37], and the nonlocal strain-gradient theory [38]. Further, the Eringen's differential theories are also derived from these integral theories subject to some conditions on the choice of the kernel [14,39], which further limits the scope of differential nonlocal theories. Additionally, the differential theories are also not well-posed leading to inconsistent softening or even paradoxical observation of stiffening influence by nonlocality [17,40]. All the models discussed above, including the fractional-order theory, involve only the classical modes of deformation and result in a softening influence of nonlocal interactions. On the other side, there exist higher-order models [41,42] and higher-grade theories [43] that also include additional modes of deformation and provide a stiffening influence of the nonlocal interactions [44].

In this study, building upon the existing geometrically nonlinear fractional-order kinematic approach to nonlocal elasticity theory, we develop a framework for the stability analysis of nonlocal slender structures. As will be shown later, the fractional-order kinematic relations allow the nonlocal effects to be accounted for on both the material and the geometric stiffness terms. The objective of the current work is two-fold. First, the conditions necessary to achieve structural stability of fractional-order nonlocal solids are derived following an energy approach. As part of this goal, we extend the classical Lagrange-Dirichlet theorem for fractional-order continua and apply it to obtain the critical loads for buckling of nonlocal structures. Note that this energy based approach to stability is possible due to the positive-definite deformation energy characteristic of the fractional-order models for nonlocal elasticity [23,32]. Second, we apply the stability theory to perform a critical load analysis for the linear buckling of fractional-order beams and plates. For this purpose, we make use of the fractional finite

element model (f-FEM) developed here for a numerical solution of the eigenvalue stability problem and to perform a parametric analysis to assess the effect of the fractional-order nonlocality on the critical buckling load.

In this paper, we begin with an introduction to the constitutive modeling of the fractional-order theory of nonlocal elasticity in §2 followed by the development of a framework of stability analysis for the fractional-order models in §3. Later, we use this framework in §4 to derive the theoretical and numerical models for nonlocal beams and plates using variational principles. Finally, we use a f-FEM approach to evaluate the critical loads corresponding to the fractional-order nonlocal structures and thereby study the influence of the long-range nonlocal interactions on the critical loads in §5.

2. Constitutive modeling for fractional-order nonlocal elasticity

In this section, we review the basic constitutive relations for the fractional-order continuum theory [6,33]. We begin with a brief review of the fractional-order kinematic relations and of the constitutive relations for nonlocal solids developed in agreement with thermodynamic principles.

Analogously to classical elasticity models, the fractional-order geometrically nonlinear Lagrangian strain tensor for nonlocal solids is given by [6,33]:

$$\overset{\alpha}{\mathbf{E}} = \frac{1}{2} \left(\nabla^{\alpha} \mathbf{U}_{X} + \nabla^{\alpha} \mathbf{U}_{X}^{T} + \nabla^{\alpha} \mathbf{U}_{X}^{T} \nabla^{\alpha} \mathbf{U}_{X} \right) \tag{1}$$

where $\mathbf{U}(\mathbf{X})$ is the Lagrangian displacement field. In the above expression, the fractional-order derivative of the displacement vector $\mathbf{U}(\mathbf{X})$ evaluated with respect to spatial coordinates $\mathbf{X} \subseteq \mathbb{R}^3$ is denoted by $\nabla^{\alpha}\mathbf{U}_{X}$. The component form for this second-order tensor is $\nabla^{\alpha}_{ij}\mathbf{U}_{X} = D^{\alpha}_{X_{j}}U_{i}$. The space-fractional derivative $D^{\alpha}_{X}\mathbf{U}(\mathbf{X})$ to the order $\alpha \in (0,1)$ is defined as [6]:

$$D_{\mathbf{X}}^{\alpha}\mathbf{U}(\mathbf{X}) = \frac{1}{2}\Gamma(2-\alpha)\left[\mathbf{L}_{A}^{\alpha-1} {}_{\mathbf{X}_{A}}^{C} D_{\mathbf{X}}^{\alpha}\mathbf{U}(\mathbf{X}) - \mathbf{L}_{B}^{\alpha-1} {}_{\mathbf{X}}^{C} D_{\mathbf{X}_{B}}^{\alpha}\mathbf{U}(\mathbf{X})\right] \tag{2}$$

where $\Gamma(\cdot)$ is the (complete) Gamma function defined over real numbers, and the expressions $_{\mathbf{X}_{A}}^{C}D_{\mathbf{X}}^{\alpha}\mathbf{U}(\mathbf{X})$ and $_{\mathbf{X}}^{C}D_{\mathbf{X}_{B}}^{\alpha}\mathbf{U}(\mathbf{X})$ are left- and right-handed Caputo spatial derivatives of the displacement field vector $\mathbf{U}(\mathbf{X})$. While the above expression is a form of the Riesz-Caputo derivative defined for $\alpha \in (0, 1)$, the fractional-order derivative $D_{\mathbf{x}}^{\alpha}\mathbf{U}(\mathbf{X})$ identically reduces to the first integer-order derivative when $\alpha = 1$. We merely note that the above definition differs from the classical Riesz fractional derivative defined in [45]. The terminals of the fractional-order RC derivative are given as $X_A = X - L_A$ and $X_B = X + L_B$. Here, L_A and L_B are length scale parameters associated with the fractional-order model for nonlocal elasticity. The domain enclosed by the terminals (X_A, X_B) defines the horizon of nonlocal influence at the point X. Note that the expressions $\mathbf{L}_A^{\alpha-1}$ and $\mathbf{L}_B^{\alpha-1}$ in the above equation ensure frame-invariance of the fractional-order continuum theory, and dimensional consistency of the fractional-order strain. These parameters are defined such that they can be, if needed, asymmetric (different on either side of a point in a fixed direction), anisotropic (different for different directions), as well as spatially-variable. This formulation generalizes alternative fractionalorder continuum formulations [46,47]. More specifically, unlike similar fractional-order continuum theories, the length scale parameters in the current formulation allow for an appropriate truncation of the length scales to address asymmetric nonlocal horizons when in presence of physical discontinuities in the domain [6]. The parameter $\frac{1}{2}\Gamma(2-\alpha)$ along with the length scales, in the RC definition, ensures frame invariance of the fractional-order strain. Further discussion regarding the geometrical meaning of fractional-order kinematic relations and the objectivity of constitutive relations developed within the framework of fractional-order continuum theory along with the physical interpretation of the fractional-order model are available in [6,32].

The integro-differential nature of the fractional-order derivative used above introduces the effect of nonlocal interactions on the elastic response, at the level of kinematics. To illustrate this aspect, the definition of the RC fractional-derivative given in Eq. (2) can be recast as:

$$D_{\mathbf{X}}^{\alpha}[\mathbf{U}(\mathbf{X})] = \int_{\mathbf{X} - \mathbf{L}_{A}}^{\mathbf{X} + \mathbf{L}_{B}} \mathcal{A}(\mathbf{X}, \boldsymbol{\xi}, \boldsymbol{\alpha}) \ D_{\boldsymbol{\xi}}^{1}[\mathbf{U}(\boldsymbol{\xi})] \ \mathrm{d}\boldsymbol{\xi} \tag{3}$$

where the kernel $A(\mathbf{X}, \boldsymbol{\xi}, \alpha)$ is the α -order power-law function connecting the point under study X and another point ξ within its domain of influence. The above mathematical statement allows the fractional derivative $D_{\mathbf{v}}^{\alpha}[\mathbf{U}(\mathbf{X})]$ to be interpreted as convolution of (integer) first-order derivative $D^1_{\mathbf{v}}[\mathbf{U}(\mathbf{X})]$ weighted by the power-law kernel $\mathcal{A}(\mathbf{X}, \boldsymbol{\xi}, \alpha)$ over the domain of influence (X_A, X_B) . The power-law kernel in the above expressions may be interpreted as the attenuation function corresponding to fractional-order model of nonlocal elasticity, analogous to the classical definition for integer-order nonlocal elasticity [20]. Note also that the power-law kernel satisfies the normalization: $\int_{\mathbf{X}_A}^{\mathbf{X}_B} A d\xi = 1$ for all the points within the solid. This condition allows recovering local response conditions under uniform field distributions [22]. The positiondependent length scales for nonlocal horizon of influence allows this condition to be satisfied for points within the solid that are close to the geometric boundaries (see [6]). We also note that the geometric definition of the fractional-order strain (and thereby the fractional-order deformation gradient tensor) may be stated as the parameter defined to capture the change of the length of an infinitesimal line in the nonlocal body. This is done by including the (nonlocal) effects of the points within the domain of influence (X_A, X_B) through the differ-integral definition of the fractional-order derivative.

The complete nonlinear expressions for the fractional-order Euler-Lagrange strain-displacement relations given in Eq. (1) can be simplified to obtain the fractional-order analogues of the von-Kármán strain-displacement relations. For a geometrically nonlinear elastic response assuming large displacement, but small numerical values for strains, the fractional-order von-Kármán strains are [33,36]:

$$\tilde{\epsilon}_{ij} = \underbrace{\frac{1}{2} \left(D_{X_j}^{\alpha} U_i + D_{X_i}^{\alpha} U_j \right)}_{\tilde{\epsilon}_{ij}(\mathbf{u})} + \underbrace{\frac{1}{2} \left(D_{X_i}^{\alpha} U_3 \ D_{X_j}^{\alpha} U_3 \right)}_{\tilde{q}_{ij}(\mathbf{u}, \mathbf{u})}, \quad i, j = 1, 2$$

$$\tag{4}$$

where U_k for k=1,2,3 are the components of the displacement field vector. More specifically, $U_3(\mathbf{X})$ corresponds the transverse component of the displacement field vector at point \mathbf{X} . Similarly, U_1 and U_2 are displacement components along x_1 and x_2 -directions, respectively. The transverse strain components (normal $\tilde{\epsilon}_{33}$ and shear $\tilde{\epsilon}_{31}$, $\tilde{\epsilon}_{32}$) are the linearized forms of their respective expressions available from Eq. (1). Here, $\tilde{\mathbf{e}}(\mathbf{u})$ and $\tilde{\mathbf{q}}(\mathbf{u},\mathbf{u})$ denote the linear and quadratic components of the von-Kármán strain.

Modeling nonlocal interactions via the kinematic relations allows the definition of localized material constitutive relations to be extended to a fractional-order continuum theory in a thermodynamically consistent manner [23]. In other terms, the tensor representing the material properties of the fractional nonlocal model maintains the same form as the classical tensor used in local elasticity. Therefore, the localized material constitutive relations provide a one-to-one correspondence between the fractional-order strain ($\tilde{\epsilon}$) and the nonlocal stress ($\tilde{\sigma}$) evaluated at a point within the solid, under the assumption of linear material constitutive relations. For the general class of hyperelastic solids with a non-dissipative response, a strictly convex functional $\mathcal{V}[\mathbf{u}(\mathbf{x})]$ referred to as the deformation energy density can be defined. The constitutive relations for the fractional-order nonlocal solid, obtained from the thermodynamic balance laws, may be written as [23]:

$$\tilde{\sigma}_{ij} = \frac{\partial \mathcal{U}(\tilde{\epsilon})}{\partial \tilde{\epsilon}_{ij}} \tag{5}$$

where the deformation energy density for a linear elastic nonlocal solid is [23]:

$$\mathcal{U}(\tilde{\epsilon}) = \frac{1}{2}\tilde{\sigma}_{ij}(\tilde{\epsilon})\ \tilde{\epsilon}_{ij} = \frac{1}{2}\ C_{ijkl}\ \tilde{\epsilon}_{ij}\ \tilde{\epsilon}_{kl} \tag{6}$$

 C_{ijkl} in the above expression is the positive-definite fourth-order elastic coefficient tensor. Note that the above expression for potential energy is positive-definite (assuming non-zero deformation) and convex in nature for a positive-definite elasticity coefficient tensor. The stability of the elastic law (material stability) for linear elastic solids follows from this strict monotonicity and positive-definite elasticity coefficient tensor. It is clear that the conditions for strong ellipticity of the elastic coefficient tensor for the fractional-order nonlocal solid simply follows from analogous results of the classical theory of elasticity. Therefore, the conditions for material stability of the nonlocal solid are also local in nature. Finally, the constitutive relations for the nonlocal stress in an isotropic solid are given as:

$$\tilde{\sigma}_{ij}(\tilde{\epsilon}) = \lambda \delta_{ij} \tilde{\epsilon}_{kk} + 2\mu \tilde{\epsilon}_{ij} \tag{7}$$

where the material elastic constants, considering isotropy, are the Lamé parameters λ and μ . The conditions for material stability of the isotropic nonlocal solid are $\lambda + (2/3)\mu > 0$ and $\mu > 0$, similarly to the classical theory of elasticity. This follows from extending the Drucker's stability postulate for nonlinear constitutive laws [48] to the stability of nonlinear fractional-order materials.

3. Stability analysis of fractional-order nonlocal structures

As noted by Hill [49], for an elastic solid the stability and uniqueness of adjacent equilibrium positions are intimately related. Hill showed that the incremental position is stable if a unique solution can be obtained for the boundary value problem at this point. This observation allows studying the stability of the adjacent equilibrium position by means of a linearized form of the nonlinear governing equations. The increments for adjacent equilibrium positions are characterized by a continuous variation of the control parameter Λ . This reduces the current analysis to a study of the stability of equilibrium positions for a continuous variation of this control parameter.

Although kinetic definitions for stability are more general, assuming non-dissipative elastic structures, we conduct the current analysis using the static stability criterion based on energy considerations. This criterion states that:

Given a displacement field $\mathbf{u} \in \mathbb{H}$, where \mathbb{H} is a Hilbert space equipped with the norm $||\mathbf{u}||$, we define the potential energy functional $\Pi[\mathbf{u}, \Lambda]$. The equilibrium point $(\mathbf{u}_e, \Lambda_e)$ is considered stable under the following assumptions:

- 1. The potential energy functional is differentiable up to the second order at $(\mathbf{u}_e, \Lambda_e)$.
- 2. The second variation $\delta^2\Pi[\mathbf{u}_e, \Lambda_e]$ is positive-definite.

The above proposition is the classical Lagrange-Dirichlet theorem which is now extended to the framework of fractional-order continuum theory. This is possible due to the thermodynamically consistent positive-definite definition for internal energy density given in Eq. (6), for the elastic deformation of a fractional-order nonlocal solid. In terms of kinetic conditions for stability, this can be interpreted as a bounded response of the nonlocal solid subject to perturbations at $(\mathbf{u}_a, \Lambda_a)$.

The condition described above for static stability translates into the positive-definite nature of the Hessian of the *potential* energy function, referred to as the *tangent* stiffness matrix. As discussed earlier, the deformation energy function for fractional-order nonlocal solid given in Eq. (6) is strictly convex. This ensures that the Hessian of the *deformation* energy density, also referred to as the *elastic* stiffness tensor, is positive-definite. However, it is worth noting that the increase of the control parameter Λ can result in a violation of the strong convexity of the *tangent* stiffness tensor. In the following, we study the conditions leading to the onset of instability upon increasing Λ and identify specific critical value Λ_c for a fractional-order solid

The total potential energy $\Pi[\mathbf{u},\Lambda]$ of a nonlocal structure occupying a domain Ω is expressed in terms of the deformation energy density $\mathcal{U}(\tilde{\epsilon}(\mathbf{u}))$, defined for nonlocal strains in Eq. (6), and the work done by external surface loads $\mathbf{f}(\Lambda)$ applied on the boundary $\partial\Omega^{\sigma}$. The expression for $\Pi[\mathbf{u},\Lambda]$ is:

$$\Pi[\mathbf{u}, \Lambda] = \int_{\Omega} \mathcal{U}(\tilde{\boldsymbol{\epsilon}}(\mathbf{u})) \, dV - \int_{\partial \Omega^{\sigma}} \mathbf{f}(\Lambda) \cdot \mathbf{u} \, dA$$
(8)

The first variation of the above defined potential energy is given as follows:

$$\delta \Pi = \int_{\Omega} \tilde{\boldsymbol{\sigma}} : \left[\tilde{\mathbf{e}}(\delta \mathbf{u}) + \tilde{\mathbf{q}}(\mathbf{u}, \delta \mathbf{u}) \right] dV - \int_{\partial \Omega^{\sigma}} \mathbf{f}(\Lambda) \cdot \delta \mathbf{u} dA = 0$$
(9)

In the derivation of the above result, we employ the expressions for deformation energy density in Eq. (6) and of the geometrically nonlinear kinematic relations in Eq. (4). As shown in [32], the solutions to the above equation $(\mathbf{u}_e, \Lambda_e)$ serve as the equilibrium points for the static response of a nonlocal solid. According to the Lagrange-Dirichlet theorem, the equilibrium state $(\mathbf{u}_e, \Lambda_e)$ is stable if $\delta^2 \Pi[\mathbf{u}_e, \Lambda_e] > 0$. For this, the second variation of the potential energy $\delta^2 \Pi$ evaluated at the equilibrium point $(\mathbf{u}_e, \Lambda_e)$ is given by:

$$\delta^{2}\Pi = \int_{\Omega} \left[\tilde{\mathbf{e}}(\delta \mathbf{u}) + \tilde{\mathbf{q}}(\mathbf{u}_{e}, \delta \mathbf{u}) \right] : \mathbf{C} : \left[\tilde{\mathbf{e}}(\delta \mathbf{u}) + \tilde{\mathbf{q}}(\mathbf{u}_{e}, \delta \mathbf{u}) \right] + \tilde{\boldsymbol{\sigma}}_{e} : \tilde{\mathbf{q}}(\delta \mathbf{u}, \delta \mathbf{u}) dV > 0$$

$$(10)$$

where $\tilde{\sigma}_e$ is the equilibrium stress evaluated at $(\mathbf{u}_e, \Lambda_e)$. Following the proposition given above, the critical state may now be identified to be the limit of the stability at which the second variation ceases to be positive definite. Thus, an equilibrium point can be considered the critical point of stability $(\mathbf{u}_e, \Lambda_e)$ if:

$$\int_{\Omega} \{ (\tilde{\mathbf{e}}(\delta \mathbf{u}) + \tilde{\mathbf{q}}(\mathbf{u}_c, \delta \mathbf{u})) : \mathbf{C} : (\tilde{\mathbf{e}}(\delta \mathbf{u}) + \tilde{\mathbf{q}}(\mathbf{u}_c, \delta \mathbf{u})) + \tilde{\boldsymbol{\sigma}}(\Lambda_c) : \tilde{\mathbf{q}}(\delta \mathbf{u}, \delta \mathbf{u}) \} \, \mathrm{d}V = 0$$
(11)

While the above equation may be solved for the critical load (Λ_c) corresponding to the *nonlinear* buckling of fractional-order nonlocal solids, in this study, we focus only on *linear* buckling. Analogous to classical approaches, we make certain assumptions to obtain the critical loads for linear buckling [50]. Firstly, in order to linearize the above nonlinear equation, we assume a proportional loading force ($\mathbf{f}(\Lambda) = \Lambda \mathbf{f}^0$, \mathbf{f}^0 being a representative force vector) and a small deformation at the critical point. This assumption results in the following linear equation:

$$\int_{\Omega} \{\tilde{\mathbf{e}}(\delta \mathbf{u}) : \mathbf{C} : (\tilde{\mathbf{e}}(\delta \mathbf{u})) + \Lambda_c \ \tilde{\sigma}^0 : \tilde{\mathbf{q}}(\delta \mathbf{u}, \delta \mathbf{u})\} \ dV = 0$$
(12)

where $\tilde{\sigma}^0$ is the stress generated in the solid by the representative force \mathbf{f}^0 . Finally, the load proportionality factor at the critical point corresponding to the *linear* buckling of nonlocal elastic solids is given by:

$$\Lambda_{c} = \min_{\mathbf{u}} \left[-\frac{\int_{\Omega} \tilde{\mathbf{e}}(\mathbf{u}) : \mathbf{C} : \tilde{\mathbf{e}}(\mathbf{u}) \, dV}{\int_{\Omega} \tilde{\mathbf{o}}^{0} : \tilde{\mathbf{q}}(\mathbf{u}, \mathbf{u}) \, dV} \right]$$
(13)

The above expression is the fractional-order analogue of the Rayleigh-Ritz coefficient for critical buckling load used in classical elasticity.

The expression of the critical buckling load in Eq. (13) allows for interesting observations. The numerator of the above expression corresponds to the general (or material) stiffness of the structure, while the denominator is referred to as the stability matrix or the geometric stiffness for the nonlocal structure. These geometric stiffness terms in the above equation are a result of the geometrically nonlinear strain-displacement relations. The jump into buckled state follows from the lower strain energy state corresponding to bending compared with axial compression at the critical point [51]. Therefore, the additional energy from external compression at the critical point causes transverse bending (or buckling) of the structure, as opposed to the axial response obtained until reaching the critical point. In this context, the energy associated to bending is characterized by the 'Material Stiffness' which includes the curvature $(D_{x_1}^2 w_0)$. The 'Geometric Stiffness' signifies the energy corresponding to axial compression captured by $(D_{x_1}^1 w_0)^2$ (von-Kármán nonlinear term in axial strain ϵ_{11}). Note that, in obtaining the critical load of the nonlocal solid using the fractional-order kinematic approach, the influence of the nonlocality is realized on both the general stiffness term as well as the geometric stiffness term. Following our discussion in the introduction, we note that this is unlike classical integer-order nonlocal theories that include the nonlocal elasticity affect only the general stiffness while the geometric stiffness terms remain identical to case of local elasticity. The implications of fractional-order kinematics in the geometric stiffness have not been previously noted in the literature.

4. Buckling of fractional-order slender nonlocal structures

In this section, we apply the above formulation to determine the critical loads of nonlocal beams and plates modeled according to the fractionalorder continuum theory. Following the procedure discussed in §3 for a general solid, we begin with geometrically nonlinear kinematic (straindisplacement) relations to derive the governing equations of equilibrium. Finally, in order to obtain the critical load for linear buckling, we linearize the system equations to setup the eigenvalue problem.

4.1. Euler-Bernoulli beams

In this study, slender beams with geometric length L and height h are chosen such that L/h > 50. The width of the beam is denoted by b. As shown in the schematic in Fig. 1, the Cartesian coordinate axis x_1 is aligned along the length of the beam, and the surface $x_3 = 0$ coincides with the mid-plane. Thus, $x_1 = 0$ and $x_1 = L$ are the longitudinal ends of the beam, while $x_3 = \pm h/2$ are the top and bottom surfaces.

For the slender beam, the following Euler-Bernoulli beam displacement theory is considered here:

$$u_1(x_1, x_3) = u_0(x_1) - x_3 \frac{\mathrm{d}w_0(x_1)}{\mathrm{d}x_1}, \quad u_3(x_1, x_3) = w_0(x_1) \tag{14}$$

where, $u_0(x_1)$ and $w_0(x_1)$ are the generalized displacement coordinates defined at a point $X_0(x_1)$ on the reference plane $x_3 = 0$. They correspond to the axial and transverse displacement fields at $X_0(x_1)$. Hereafter, the functional dependence on the axial coordinate x_1 is implied and not mentioned for the sake of brevity. In the following, the fractional-order geometrically nonlinear strains evaluated using the von-Kármán kinematic (strain-displacement) relations in Eq. (4) are:

$$\tilde{\epsilon}_{11} = D_{x_1}^{\alpha} u_0 - x_3 D_{x_1}^{\alpha} \left[\frac{\mathrm{d}w_0}{\mathrm{d}x_1} \right] + \frac{1}{2} \left(D_{x_1}^{\alpha} w_0 \right)^2 \tag{15}$$

where $D_{x_1}^{\alpha} \square$ is a concise notation for the RC fractional-order derivative $x_1 - l_A D_{x_1 + l_B}^{\alpha}$ in the x_1 direction. Using Eq. (7), the axial stress in the nonlocal beam is obtained as:

$$\tilde{\sigma}_{11}(x_1) = E\tilde{\epsilon}_{11}(x_1) \tag{16}$$

where E is the Young's modulus for the isotropic solid. Non-zero transverse shear stresses may be neglected under the slender beam assumption. As shown in Eq. (8), the nonlinear fractional-order governing differential equations of equilibrium of the nonlocal beam may be derived following the principle of minimum potential energy: $\delta\Pi = 0$. They are given as follows [33]:

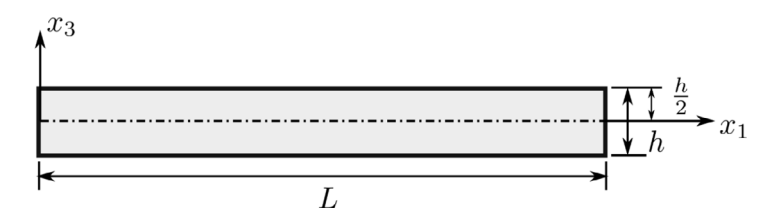


Fig. 1. Schematic of the isotropic beam illustrating the Cartesian coordinate axes and a few geometric parameters.

$$\mathfrak{D}_{+}^{\alpha} N_{11}(x_1) + F_1(x_1) = 0 \quad \forall x_1 \in (0, L) \tag{17a}$$

$$D_{x_1}^1 \left[\mathfrak{D}_{x_1}^{\alpha} M_{11}(x_1) \right] + \mathfrak{D}_{x_1}^{\alpha} \left[N_{11}(x_1) D_{x_1}^{\alpha} \left[w_0 \right] \right] + F_3(x_1) = 0 \ \, \forall \, x_1 \in (0,L) \tag{17b}$$

where $F_1(x_1)$ and $F_3(x_1)$ are the distributed forces acting on the nonlocal beam. The essential and natural boundary conditions for the current study are:

$$N_{11}(x_1 = L) = -N_0 \text{ and } \delta u_0(x_1 = 0) = 0$$
 (18a)

$$M_{11}(x_1) = 0 \text{ or } \delta \left[D_{x_1}^1 w_0 \right] = 0 \ \forall \ x_1 \in \{0, L\}$$
 (18b)

$$D_{x_1}^1 M_{11}(x_1) + N_{11}(x_1) D_{x_1}^1 [w_0] = 0 \text{ or } \delta w_0 = 0 \ \forall \ x_1 \in \{0, L\}$$
 (18c)

where $N_0(>0)$ is the magnitude of the externally applied compressive surface loads along x_1 at the free end. In Eqs. (17) and (18), $N_{11}(x_1)$ and $M_{11}(x_1)$ are the stress resultants associated with axial extension and bending of the nonlocal beam. They are defined as follows:

$$N_{11}(x_1) = \int_{-b/2}^{b/2} \int_{-h/2}^{h/2} \tilde{\sigma}_{11}(x_1, x_3) \, \mathrm{d}x_3 \, \mathrm{d}x_2 \tag{19a}$$

$$M_{11}(x_1) = \int_{-b/2}^{b/2} \int_{-h/2}^{h/2} x_3 \,\tilde{\sigma}_{11}(x_1, x_3) \, \mathrm{d}x_3 \, \mathrm{d}x_2 \tag{19b}$$

The expression $\mathfrak{D}_{x_1}^{a}(\cdot)$ that appears in Eq. (18) denotes the following Reisz-Riemann Liouville (R-RL) fractional derivative:

$$\mathfrak{D}_{x_1}^{\alpha}(\cdot)f(x_1) = \frac{1}{2}\Gamma(2-\alpha) \left[l_B^{\alpha-1} \binom{RL}{x_1-l_R} D_{x_1}^{\alpha} f(x_1) \right) - l_A^{\alpha-1} \binom{RL}{x_1} D_{x_1+l_A}^{\alpha} f(x_1) \right] \tag{20}$$

where α is the fractional-order, and $f(x_1)$ is an arbitrary function. It may be noted that the above expression is a Riemann Liouville analogue of the previously encountered Caputo-based Reisz fractional derivative in Eq. (2). In the above expression, the terms $\frac{RL}{x_1-l_B}D^{\alpha}_{x_1}f(x_1)$ and $\frac{RL}{x_1}D^{\alpha}_{x_1+l_A}f(x_1)$ are the left- and right-handed fractional-order derivatives of $f(x_1)$ to the order α evaluated using Riemann Liouville formalism, respectively. The fractional-order R-RL derivative $\mathfrak{D}^{\alpha}_{x_1}(\cdot)$ is carried out with respect to the axial coordinate (x_1) over the interval (x_1-l_B,x_1+l_A) . This is unlike the RC fractional derivative $D^{\alpha}_{x_1}(\cdot)$ defined over the interval (x_1-l_A,x_1+l_B) .

The self-adjoint nature of the linear operators in the governing equations follows from the convexity of the deformation energy density used in their derivation. The proof of this property is provided in [32]. The positive-definite definition of the deformation energy density given in Eq. (6) and the self-adjoint fractional operators in the governing equations result in a consistent softening of the structure upon inclusion of the nonlocal interactions [32,33].

For the current study, concerning the identification of the critical load for *linear* buckling, we linearize the nonlinear fractional-order governing equations given in Eq. (18), under the assumptions of proportional loading and small deformations at the critical point as discussed in §3. Considering the case without externally applied distributed loads (i.e. $F_1(x_1) = F_3(x_1) = 0$), the linearized fractional-order governing equations of equilibrium for the Euler-Bernoulli nonlocal beam before the onset of buckling are obtained as:

$$\mathfrak{D}_{x_1}^{\alpha} N_{11}(x_1) = 0 \ \forall x_1 \in (0, L)$$
 (21a)

$$D_{x_{1}}^{1}\left[\mathfrak{D}_{x_{1}}^{\alpha}M_{11}(x_{1})\right] + \overline{N}_{0}\mathfrak{D}_{x_{1}}^{\alpha}\left(D_{x_{1}}^{\alpha}\left[w_{0}\right]\right) = 0 \ \ \forall \ x_{1} \in (0,L) \tag{21b}$$

where the constant \overline{N}_0 is the in-plane stress-resultant along x_1 at the onset of buckling. In the derivation of the above equations, it is assumed that the beam is straight $(w_0(x_1) = 0)$ before buckling. Solving the linearized fractional-order governing equation for the axial response given in Eq. (21a) and subject to uniform edge loading N_0 expressed via natural boundary conditions in Eq. (18a), we obtain the in-plane stress resultants $\overline{N}_0 = -N_0$. A detailed derivation of the above results in provided in Appendix A.1. From the above equations, it is clear that the elastic response in the x_1 and x_3 -directions are decoupled. Therefore, we only proceed with solving the linearized governing equation for the transverse direction given in Eq. (21b). This is the eigenvalue problem that governs the onset of buckling in a nonlocal beam subject to compressive axial force N_0 . The smallest value of the N_0 for which instability sets in is the critical load.

Obtaining analytical solutions to the eigenvalue problem involving fractional-order governing equations is not a trivial task and typically not possible. Thus, we employ a numerical solution based on the f-FEM method developed in [32]. Using the method of weighted residuals, the following mathematical expression is equivalent to the governing differential equations in Eq. (21b):

$$\int_{0}^{L} \left(D_{x_{1}}^{1} \left[\mathfrak{D}_{x_{1}}^{\alpha} M_{11}(x_{1}) \right] - N_{0} \mathfrak{D}_{x_{1}}^{\alpha} \left[D_{x_{1}}^{\alpha} w_{0} \right] \right) \delta w_{0} \, \mathrm{d}x_{1} = 0 \tag{22}$$

where a variation of the transverse displacement field δw_0 is chosen to be the weight function. Employing integration by-parts in the above expressions we derive the following weak-form equivalent of the governing equation [32]:

$$\int_{0}^{L} \frac{Eh^{3}}{12} \left(D_{x_{1}}^{\alpha} \left[\frac{\mathrm{d}w_{0}}{\mathrm{d}x_{1}} \right] \right)^{2} \mathrm{d}x_{1} - N_{0} \int_{0}^{L} \left(D_{x_{1}}^{\alpha} w_{0} \right)^{2} \mathrm{d}x_{1} = 0 \tag{23}$$

Using a finite element approximation for the transverse displacement field in the above equation, we arrive at the following set of algebraic equations:

$$[K_T^b]\{\Delta^b\} = \{0\} \tag{24a}$$

where

$$[K_T^b] = \underbrace{\int_0^L \frac{Eh^3}{12} [\tilde{B}_{\mathcal{H},11}]^T [\tilde{B}_{\mathcal{H},11}] \, \mathrm{d}x_1}_{[K^b]: \text{ Material stiffness}} - N_0 \underbrace{\int_0^L [\tilde{B}_{\mathcal{H},1}]^T [\tilde{B}_{\mathcal{H},1}] \, \mathrm{d}x_1}_{[G^b]: \text{ Geometric stiffness}}$$
(24b)

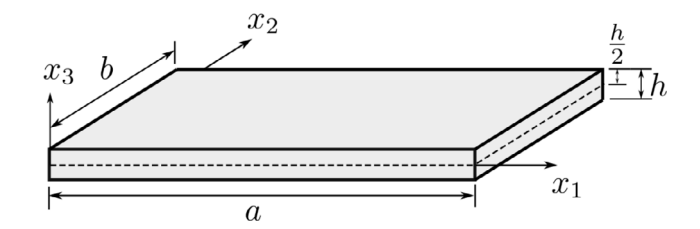


Fig. 2. Schematic of the isotropic plate depicting the Cartesian coordinate axes and relevant geometric parameters.

is the tangent stiffness matrix. The strain-displacement approximation matrices $[\tilde{B}_{H,1}]$ and $[\tilde{B}_{H,1}]$ used in the above equation are fractional-order in nature and their expressions are provided in Appendix A.2. It is evident from the expression of the geometric stiffness matrix in Eq. (24b) that the modeling of nonlocal response via the fractional-order kinematic approach effects a change in the geometric stiffness of the solid in addition to the material stiffness, as also discussed in §3. This is unlike classical integer-order approaches to nonlocal elasticity where the geometric stiffness matrix is still local in nature. Note that, in the above derivation, we employed the following approximation for the transverse displacement field:

$$\{w_0(x_1)\} = [\mathcal{H}(x_1)]\{\Delta_{\rho}^k(x_1)\} \tag{24c}$$

where $[\mathcal{H}(x_1)]$ are the one-dimensional C^1 (Hermite) approximation functions, and:

$$\{\Delta_e^b\}^T = \left[w_0^i \quad \frac{\mathrm{d}w_0^i}{\mathrm{d}x_1}\right]_{i=1}^{N_e} \tag{24d}$$

is the element nodal vector of the generalized displacement coordinates for the N_e -noded element.

4.2. Kirchhoff plates

The methodology outlined above is now extended to a thin plate. As shown in the schematic given in Fig. 2, the length and breadth of the plate are a and b, respectively, and the thickness b is chosen such that b < a/50. Further, for the Cartesian coordinate system considered here (see Fig. 2), a < a/50 is the mid-plane for the plate, and a < a/50 coincide with the transverse free faces of the plate. We consider the displacement field distribution according to the Kirchhoff plate theory:

$$u_1(\mathbf{X}) = u_0(\mathbf{X}_0) - x_3 \frac{\partial w_0(\mathbf{X}_0)}{\partial x_1}, \quad u_2(\mathbf{X}) = v_0(\mathbf{X}_0) - x_3 \frac{\partial w_0(\mathbf{X}_0)}{\partial x_2}, \quad u_3(\mathbf{X}) = w_0(\mathbf{X}_0)$$
 (25)

where $u_0(\mathbf{X}_0)$, $v_0(\mathbf{X}_0)$, and $w_0(\mathbf{X}_0)$ are the generalized displacement coordinates evaluated at a point $\mathbf{X}_0(x_1,x_2)=\mathbf{X}(x_1,x_2,0)$ (on the reference plane $x_3=0$). The expressions for the fractional-order geometrically nonlinear strains evaluated following the von-Kármán strain-displacement relations given in Eq. (4) are:

$$\tilde{\epsilon}_{11} = D_{x_1}^{\alpha} u_0 - x_3 D_{x_1}^{\alpha} \left[\frac{\partial w_0}{\partial x_1} \right] + \frac{1}{2} \left(D_{x_1}^{\alpha} w_0 \right)^2 \tag{26a}$$

$$\tilde{e}_{22} = D_{x_2}^{\alpha} v_0 - x_3 D_{x_2}^{\alpha} \left[\frac{\partial w_0}{\partial x_2} \right] + \frac{1}{2} \left(D_{x_2}^{\alpha} w_0 \right)^2 \tag{26b}$$

$$\tilde{\gamma}_{12} = 2\tilde{\epsilon}_{12} = \left(D_{x_1}^{\alpha} v_0 + D_{x_2}^{\alpha} u_0\right) - x_3 \left(D_{x_1}^{\alpha} \left[\frac{\partial w_0}{\partial x_1}\right] + D_{x_2}^{\alpha} \left[\frac{\partial w_0}{\partial x_2}\right]\right) + \left(D_{x_1}^{\alpha} w_0 D_{x_2}^{\alpha} w_0\right)$$
(26c)

Here, $D_{x_1}^{\alpha} \equiv_{x_1-l_{A_1}} D_{x_1+l_{B_1}}^{\alpha}$ and $D_{x_2}^{\alpha} \equiv_{x_2-l_{A_2}} D_{x_2+l_{B_2}}^{\alpha}$ denote the RC fractional derivatives along x_1 and x_2 . The domains $(x_1-l_{A_1},x_1+l_{B_1})$ and $(x_2-l_{A_2},x_2+l_{B_2})$ provide the horizon of influence for the point $\mathbf{X}_0(x_1,x_2)$ along the x_1 and x_2 -directions. The length scales l_{A_i} and l_{B_i} (i=1,2) are the nonlocal length scales in x_i -direction. Using Eq. (7), the nonlocal stresses in the isotropic plate are obtained as:

$$\tilde{\sigma}_{11} = \frac{E}{1 - v^2} \left(\tilde{\epsilon}_{11} + v \tilde{\epsilon}_{22} \right) \tag{27a}$$

$$\tilde{\sigma}_{22} = \frac{E}{1 - v^2} \left(v \tilde{\epsilon}_{11} + \tilde{\epsilon}_{22} \right) \tag{27b}$$

$$\tilde{\sigma}_{12} = \frac{E}{2(1+\nu)}\tilde{\gamma}_{12} \tag{27c}$$

where E is the Young's modulus and ν is the Poisson's ratio of the isotropic solid.

As mentioned previously in the case of fractional-order Euler-Bernoulli beam, the fractional-order governing differential equations of equilibrium of the nonlocal Kirchhoff plate are derived following the principle of minimum potential energy. They are given as [36]:

$$\mathfrak{D}_{x_1}^{\alpha} N_{11} + \mathfrak{D}_{x_2}^{\alpha} N_{12} + F_1 = 0 \tag{28a}$$

$$\mathfrak{D}_{x_1}^{u} N_{12} + \mathfrak{D}_{x_2}^{u} N_{22} + F_2 = 0 \tag{28b}$$

$$D_{x_{1}}^{1}\left[\mathfrak{D}_{x_{1}}^{\alpha}M_{11}+\mathfrak{D}_{x_{2}}^{\alpha}M_{12}\right]+D_{x_{2}}^{1}\left[\mathfrak{D}_{x_{1}}^{\alpha}M_{12}+\mathfrak{D}_{x_{2}}^{\alpha}M_{22}\right]+\mathfrak{D}_{x_{1}}^{\alpha}(N_{11}D_{x_{1}}^{\alpha}w_{0}+N_{12}D_{x_{2}}^{\alpha}w_{0})+\mathfrak{D}_{x_{2}}^{\alpha}(N_{12}D_{x_{1}}^{\alpha}w_{0}+N_{22}D_{x_{2}}^{\alpha}w_{0})+F_{3}=0 \tag{28c}$$

where F_i ($i = \{1, 2, 3\}$) are externally applied distributed forces, and N_{\square} and M_{\square} are, respectively, the stress resultants associated with in-plane and bending response of the mid-plane evaluated at \mathbf{X}_0 . They are evaluated using the nonlocal stresses given in Eq. (27) as follows:

$$N_{ij} = \int_{-h/2}^{h/2} \tilde{\sigma}_{ij} \, dx_3, \quad M_{ij} = \int_{-h/2}^{h/2} x_3 \, \tilde{\sigma}_{ij} \, dx_3$$
 (29)

where $i, j \in \{1, 2\}$. The boundary conditions necessary to solve the governing equations given above are:

$$\forall x_2 \mid x_1 = \{0, a\} : \begin{cases} \delta u_0 = 0 & \text{or} \quad N_{11} = -N_1 \\ \delta v_0 = 0 & \text{or} \quad N_{12} = 0 \\ \delta w_0 = 0 & \text{or} \quad N_{12} = 0 \end{cases}$$

$$\delta w_0 = 0 & \text{or} \quad D_{x_1}^1 M_{11} + 2D_{x_2}^1 M_{12} + N_{11} D_{x_1}^1 w_0 + N_{12} D_{x_2}^1 w_0 = 0$$

$$\delta D_{x_1}^1 w_0 = 0 & \text{or} \quad M_{11} = 0$$

$$(30a)$$

$$\forall x_1 \mid x_2 = \{0, b\} : \begin{cases} \delta u_0 = 0 & \text{or} \quad N_{12} = 0\\ \delta v_0 = 0 & \text{or} \quad N_{22} = -N_2\\ \delta w_0 = 0 & \text{or} \quad D_{x_2}^1 M_{22} + 2D_{x_1}^1 M_{12} + N_{12}D_{x_1}^1 w_0 + N_{22}D_{x_2}^1 w_0 = 0\\ \delta D_{x_2}^1 w_0 = 0 & \text{or} \quad M_{22} = 0 \end{cases}$$
(30b)

where $N_1(>0)$ and $N_2(>0)$ are the magnitudes of the externally applied uniform compressive surface loads at the free ends in the x_1 and x_2 -directions, respectively. Recall that the terms $\mathfrak{D}_{x_1}^{\alpha}(\cdot)$ and $\mathfrak{D}_{x_2}^{\alpha}(\cdot)$ in the above equations are the R-RL fractional-order derivative with respect to x_1 and x_2 . The expressions for these derivatives follow from the definition for R-RL fractional derivative given in Eq. (20).

In order to obtain the critical load for *linear* buckling, the above given fractional-order nonlinear governing equations of equilibrium are linearized following the methodology outlined in §3 for general solids and employed for analysis of beams in §4.1. The linearized governing equations for the Kirchhoff plates before the onset of buckling, assuming externally applied distributed loads to be absent, are:

$$\mathfrak{D}_{x_1}^{a} N_{11} + \mathfrak{D}_{x_2}^{a} N_{12} = 0 \tag{31a}$$

$$\mathfrak{D}_{x_1}^a N_{12} + \mathfrak{D}_{x_2}^a N_{22} = 0 \tag{31b}$$

$$D_{x_{1}}^{1}\left[\mathfrak{D}_{x_{1}}^{\alpha}M_{11}+\mathfrak{D}_{x_{2}}^{\alpha}M_{12}\right]+D_{x_{2}}^{1}\left[\mathfrak{D}_{x_{1}}^{\alpha}M_{12}+\mathfrak{D}_{x_{2}}^{\alpha}M_{22}\right]+\overline{N}_{11}\mathfrak{D}_{x_{1}}^{\alpha}\left[D_{x_{1}}^{\alpha}w_{0}\right]+\overline{N}_{12}\mathfrak{D}_{x_{1}}^{\alpha}\left[D_{x_{2}}^{\alpha}w_{0}\right]+\overline{N}_{12}\mathfrak{D}_{x_{2}}^{\alpha}\left[D_{x_{1}}^{\alpha}w_{0}\right]+\overline{N}_{12}\mathfrak{D}_{x_{2}}^{\alpha}\left[D_{x_{1}}^{\alpha}w_{0}\right]+\overline{N}_{12}\mathfrak{D}_{x_{2}}^{\alpha}\left[D_{x_{1}}^{\alpha}w_{0}\right]+\overline{N}_{12}\mathfrak{D}_{x_{2}}^{\alpha}\left[D_{x_{1}}^{\alpha}w_{0}\right]+\overline{N}_{12}\mathfrak{D}_{x_{2}}^{\alpha}\left[D_{x_{1}}^{\alpha}w_{0}\right]+\overline{N}_{12}\mathfrak{D}_{x_{2}}^{\alpha}\left[D_{x_{1}}^{\alpha}w_{0}\right]+\overline{N}_{12}\mathfrak{D}_{x_{2}}^{\alpha}\left[D_{x_{1}}^{\alpha}w_{0}\right]+\overline{N}_{12}\mathfrak{D}_{x_{2}}^{\alpha}\left[D_{x_{1}}^{\alpha}w_{0}\right]+\overline{N}_{12}\mathfrak{D}_{x_{2}}^{\alpha}\left[D_{x_{1}}^{\alpha}w_{0}\right]+\overline{N}_{12}\mathfrak{D}_{x_{2}}^{\alpha}\left[D_{x_{1}}^{\alpha}w_{0}\right]+\overline{N}_{12}\mathfrak{D}_{x_{2}}^{\alpha}\left[D_{x_{1}}^{\alpha}w_{0}\right]+\overline{N}_{12}\mathfrak{D}_{x_{2}}^{\alpha}\left[D_{x_{1}}^{\alpha}w_{0}\right]+\overline{N}_{12}\mathfrak{D}_{x_{2}}^{\alpha}\left[D_{x_{1}}^{\alpha}w_{0}\right]+\overline{N}_{12}\mathfrak{D}_{x_{2}}^{\alpha}\left[D_{x_{1}}^{\alpha}w_{0}\right]+\overline{N}_{12}\mathfrak{D}_{x_{2}}^{\alpha}\left[D_{x_{1}}^{\alpha}w_{0}\right]+\overline{N}_{12}\mathfrak{D}_{x_{2}}^{\alpha}\left[D_{x_{1}}^{\alpha}w_{0}\right]+\overline{N}_{12}\mathfrak{D}_{x_{2}}^{\alpha}\left[D_{x_{1}}^{\alpha}w_{0}\right]+\overline{N}_{12}\mathfrak{D}_{x_{2}}^{\alpha}\left[D_{x_{1}}^{\alpha}w_{0}\right]+\overline{N}_{12}\mathfrak{D}_{x_{2}}^{\alpha}\left[D_{x_{1}}^{\alpha}w_{0}\right]+\overline{N}_{12}\mathfrak{D}_{x_{2}}^{\alpha}\left[D_{x_{1}}^{\alpha}w_{0}\right]+\overline{N}_{12}\mathfrak{D}_{x_{2}}^{\alpha}\left[D_{x_{1}}^{\alpha}w_{0}\right]+\overline{N}_{12}\mathfrak{D}_{x_{2}}^{\alpha}\left[D_{x_{1}}^{\alpha}w_{0}\right]+\overline{N}_{12}\mathfrak{D}_{x_{2}}^{\alpha}\left[D_{x_{1}}^{\alpha}w_{0}\right]+\overline{N}_{12}\mathfrak{D}_{x_{2}}^{\alpha}\left[D_{x_{1}}^{\alpha}w_{0}\right]+\overline{N}_{12}\mathfrak{D}_{x_{2}}^{\alpha}\left[D_{x_{1}}^{\alpha}w_{0}\right]+\overline{N}_{12}\mathfrak{D}_{x_{2}}^{\alpha}\left[D_{x_{1}}^{\alpha}w_{0}\right]+\overline{N}_{12}\mathfrak{D}_{x_{2}}^{\alpha}\left[D_{x_{1}}^{\alpha}w_{0}\right]+\overline{N}_{12}\mathfrak{D}_{x_{2}}^{\alpha}\left[D_{x_{1}}^{\alpha}w_{0}\right]+\overline{N}_{12}\mathfrak{D}_{x_{2}}^{\alpha}\left[D_{x_{1}}^{\alpha}w_{0}\right]+\overline{N}_{12}\mathfrak{D}_{x_{2}}^{\alpha}\left[D_{x_{1}}^{\alpha}w_{0}\right]+\overline{N}_{12}\mathfrak{D}_{x_{2}}^{\alpha}\left[D_{x_{1}}^{\alpha}w_{0}\right]+\overline{N}_{12}\mathfrak{D}_{x_{2}}^{\alpha}\left[D_{x_{1}}^{\alpha}w_{0}\right]+\overline{N}_{12}\mathfrak{D}_{x_{2}}^{\alpha}\left[D_{x_{1}}^{\alpha}w_{0}\right]+\overline{N}_{12}\mathfrak{D}_{x_{2}}^{\alpha}\left[D_{x_{1}}^{\alpha}w_{0}\right]+\overline{N}_{12}\mathfrak{D}_{x_{2}}^{\alpha}\left[D_{x_{1}}^{\alpha}w_{0}\right]+\overline{N}_{12}\mathfrak{D}_{x_{2}}^{\alpha}\left[D_{x_{1}}^{\alpha}w_{0}\right]+\overline{N}_{12}\mathfrak{D}_{x_{2}}^{\alpha}\left[D_{x_{1}}^{\alpha}w_{0}\right]+\overline{N}_{12}\mathfrak{D}_{x_{2}}^{\alpha}\left[D_{x_{1}}^{\alpha}w_{0}\right$$

where \overline{N}_{\square} are the in-plane stress-resultants before the onset of buckling. We assume two separate cases: (1) uniaxial compression where the plate is subject to externally applied distributed surface loads N_1 on the transverse faces at $x_1 = 0$ and $x_1 = a$; (2) biaxial compression where the plate is subject to N_1 on faces $x_1 = 0$, $x_1 = 0$, $x_2 = 0$, $x_3 = 0$. In the absence of external shear loads, the linearized fractional-order governing differential equation corresponding to the transverse displacement of the nonlocal plate is given as:

$$D_{x_1}^1 \left[\mathfrak{D}_{x_1}^{\alpha} M_{11} + \mathfrak{D}_{x_2}^{\alpha} M_{12} \right] + D_{x_2}^1 \left[\mathfrak{D}_{x_1}^{\alpha} M_{12} + \mathfrak{D}_{x_2}^{\alpha} M_{22} \right] - N_1 \mathfrak{D}_{x_1}^{\alpha} \left[D_{x_1}^{\alpha} w_0 \right] - N_2 \mathfrak{D}_{x_2}^{\alpha} \left[D_{x_2}^{\alpha} w_0 \right] = 0$$

$$(32)$$

The above equation corresponds to the biaxial compression, and may be reduced to uniaxial compression by setting, as an example, $N_2 = 0$. Note that the in-plane stress resultants \overline{N}_{11} and \overline{N}_{22} in Eq. (31c) are equal to the magnitude of the uniform edge loads N_1 and N_2 , respectively. This follows from solving the in-plane governing equations given in Eq. (31) subject to boundary conditions given in Eq. (30).

As in the previously encountered case of fractional-order beams, we employ the method of weighted residuals to express the following mathematical statement as equivalent to the fractional-order governing equation in Eq. (32):

Integral operations to reduce the above statement into the weak equation for Eq. (32), and finite element approximations for the displacement field variables gives the following algebraic equations of equilibrium:

$$[K_T^p]\{\Delta^p\} = \{0\}$$
 (34a)

where the tangent stiffness matrix $[K_T^p]$ is given as

$$[K_T^p] = [K^p] - N_1[G_1^p] - N_2[G_2^p] \tag{34b}$$

Here, $[K^p]$ is the bending stiffness matrix

$$[K^{p}] = \int_{0}^{a} \int_{0}^{b} \frac{Eh^{3}}{12(1-v^{2})} \left([\tilde{B}_{H,11}]^{T} ([\tilde{B}_{H,11}] + v \ [\tilde{B}_{H,22}]) + [\tilde{B}_{H,22}]^{T} ([\tilde{B}_{H,22}] + v \ [\tilde{B}_{H,11}]) \right) + \frac{Eh^{3}}{24(1+v)} \left([\tilde{B}_{H,12}] + [\tilde{B}_{H,21}] \right)^{T} \left([\tilde{B}_{H,12}] + [\tilde{B}_{H,21}] \right) dx_{1} dx_{2}$$

$$(34c)$$

and

$$[G_1^p] = \int_0^a \int_0^b [\tilde{B}_{H,1}]^T [\tilde{B}_{H,1}] dx_1 dx_2 \quad [G_2^p] = \int_0^a \int_0^b [\tilde{B}_{H,2}]^T [\tilde{B}_{H,2}] dx_1 dx_2$$
(34d)

are the geometric stiffness matrices of the nonlocal Kirchhoff plate for compression along x_1 and x_2 directions, respectively. Note the effect of the fractional-order nonlocality on the geometric stiffness matrices via the fractional-order strain-displacement approximation matrices $[\tilde{B}_{\mathcal{H},\square}]$. In the derivation of the algebraic equations of equilibrium, we employed the following approximation for the transverse displacement field:

$$\{w_0(x_1, x_2)\} = [\mathcal{H}(x_1, x_2)]\{\Delta^p_{\sigma}(x_1, x_2)\} \tag{34e}$$

where $[\mathcal{H}(x_1, x_2)]$ are the two-dimensional C^1 (Hermite) approximation functions. The element nodal vector is expressed as:

$$\{\Delta_e^p\}^T = \left[w_0^i \quad \frac{\partial w_0}{\partial x_1}^i \quad \frac{\partial w_0}{\partial x_2}^i \quad \frac{\partial^2 w_0}{\partial x_1 \partial x_2}^i\right]_{i=1}^{N_e} \tag{34f}$$

and includes the generalized displacement coordinates for the N_e -noded element.

5. Results and discussion

We report here the results of numerical simulations conducted to study the effect of long-range interactions, modeled via fractional-order continuum theory, over the critical load of slender structures. More specifically, the f-FEM models for the Euler-Bernoulli nonlocal beam in Eq. (24) and the Kirchhoff nonlocal plate in Eq. (34) are solved for the critical load to study the influence of the fractional-order and the nonlocal length scales. The material properties of the isotropic solid are considered as follows: E = 30 MPa and v = 0.3. The nonlocal horizon is assumed to be symmetric for all those points that are sufficiently far from the boundaries. In other terms, the length scales on both sides of the point of interest are assumed to be equal. For a beam this condition translates to $I_A = I_B = I_f$, while for a plate it means $I_{A_1} = I_{B_1} = I_{A_2} = I_{B_2} = I_f$. Clearly, the symmetry of the nonlocal horizons is broken when considering points whose distance from the boundary (in a given direction) is smaller than I_f . In this latter case, appropriate truncation of the length scales is performed as indicated in the schematic of Fig. 3. This asymmetry in the length scales, for points close to the external boundaries, is achieved via the independent definitions of the length scales I_A and I_B in Eq. (2). This aspect generalizes the fractional-order continuum theory with respect to other formulations [31]. In the subsequent studies, we carry out numerical analyses and provide the results for different choices of fractional-order constitutive parameters. Note that the choice of the fractional-order α is always chosen to be greater than 0.5. This choice follows from a loss of consistency in nonlocal elastic behavior caused by excessive softening when $\alpha < 0.5$ [32,33]. A detailed explanation of this behavior along with the physical rationale is available in [32].

5.1. Beams

In line with the assumptions for the Euler-Bernoulli beam displacement theory, we choose a thin beam with aspect ratio L/h = 100 for the current study. The width of the beam was chosen as $2 \times h$. The critical loads reported here were non-dimensionalized as follows [50]:

$$\overline{N}_0 = N_0 \times \frac{L^2}{\pi^2 E I} \tag{35}$$

Before presenting the results for the critical loads, we make an important remark on the convergence of the discretized numerical model. As discussed in [52], numerical convergence of the f-FEM requires accurate approximation of the convolution integral corresponding to the nonlocal interactions. This is ensured by considering a suitable choice of the 'dynamic rate of convergence', defined as $\mathcal{N}^{inf} = l_f/l_e$, where l_e is the size of the uniform FE mesh. For this purpose, the convergence study of the 1D f-FEM conducted for different choices of α and l_f is reported in Table 1. The study illustrates the excellent convergence of the normalized eigenvalues that achieve differences of <1% between successive refinements of the FE mesh. Following these results, we used $N^{inf} = 24$ for all the simulations presented in this section.

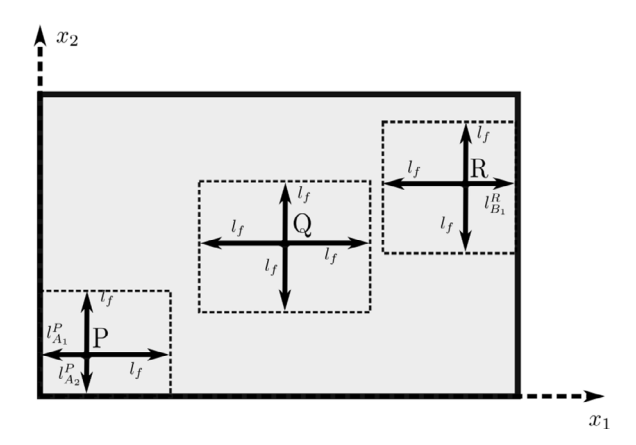


Fig. 3. Illustration of position dependent length scales for three different points (P,Q, and R) in the isotropic domain. Note the symmetry in length scales for a point Q sufficiently within the plate, unlike points P and R that are close to the boundaries.

Table 1 1D f-FEMI mesh convergence study. Non-dimensional critical load of a doubly clamped beam for different values of the constitutive parameters α and l_f . In all cases, $N^{inf}=24$ guarantees a difference between successive refinements within 1%.

Fractional Horizon		fractional-	fractional-order, α							
Length, l_f	N^{inf}	$\alpha = 1.0$	$\alpha = 0.9$	$\alpha = 0.8$	$\alpha = 0.7$					
$l_f = 0.2L$	12	4	3.9574	3.9374	3.9200					
	18	4	3.9529	3.9291	3.9072					
	24	4	3.9514	3.9251	3.8979					
	30	4	3.9506	3.9224	3.8908					
$l_f = 0.6L$	12	4	3.7216	3.3789	2.8594					
	24	4	3.7238	3.3840	2.8777					
	36	4	3.7246	3.3871	2.8817					
	48	4	3.7250	3.3882	2.8817					
$l_f = L$	12	4	3.8460	3.6969	3.4806					
,	24	4	3.8484	3.7116	3.5216					
	36	4	3.8497	3.7182	3.5389					
	30	4	3.8504	3.7215	3.5466					

Table 2Critical loads for beams subject to various boundary conditions. Results are non-dimensionalized following Eq. (35) and compared to study the effect of fractional theory constitutive parameters. Recall that SS stands for simply supported, CC for doubly clamped and CF for cantilever beam (one end clamped and other end free).

	SS				CC				CF			
α	1.0	0.9	0.8	0.7	1.0	0.9	0.8	0.7	1.0	0.9	0.8	0.7
,			0.998							0.259		0.315
$l_f = 0.6L$ $l_f = 0.8L$										0.261 0.260	0.289	0.330 0.320
$l_f = L$	1.000	1.140	1.255	1.319	4.000	3.848	3.712	3.522	0.250	0.259	0.282	0.305

The critical loads of fractional-order beams subject to simply supported (SS), doubly clamped (CC), and cantilever (CF) boundary conditions at $x_1 = 0$, L are tabulated in Table 2 for various fractional-order parameters (α and l_f). A non-monotonic variation of the critical load with increasing degree of nonlocality, obtained by reducing α and increasing l_f , is clearly evident from the table. This observation is unlike the monotonous reduction in critical load noted from similar studies based on classical integer-order nonlocal theories [12,13,21,24]. This difference is a direct result of the effect of the nonlocal response on the geometric stiffness and it is further discussed in the following.

Recall that the eigenvalue problem in Eq. (24b) involves two matrices representing the material stiffness $[K^b]$ and the geometric stiffness $[G^b]$. The effect of nonlocal interactions on the material stiffness term will be referred to as the *material nonlocality*. This implies the influence of long-range interactions on the structural rigidity (i.e. the propensity to oppose deformation) of the nonlocal solid. Similarly, we denote the nonlocal effects on the geometric stiffness term as the *geometric nonlocality*. As discussed in §3, contrary to the classical or the integer-order approaches to nonlocal elasticity, the critical load of a nonlocal solid evaluated via fractional-order kinematic relations affects both the material and geometric stiffness terms. With the increasing degree of nonlocality, both these stiffness terms are reduced. The decrease in material stiffness (often referred to as softening effect) as a result of the fractional-order kinematics was already documented in [32,33], and is in agreement with studies on classical strain-based integral models of nonlocal elasticity. The reduction of the geometric stiffness due to fractional-order kinematics was not reported in either the fractional- or integer-order studies. We merely note that, with regards to the fractional-order studies [32,33,35,36], the effect of the nonlocality on the geometric stiffness was not reported simply because of the nature of the problems (static and free vibration response) treated in the same studies. Recall however that, the constitutive modeling of the slender structures in this study and the other fractional-order studies in [32,33,35,36] is still the same. In this regard, as evident from Eq. (13) (repeated below), the reducing material stiffness (numerator) would result in decreasing the critical load, and the reducing geometric stiffness (denominator) would result in increasing critical load. It follows that the effect of an increasing degree of nonlocality on the critical load is non-monotonic due to an interp

$$\Lambda_{c} = \min_{\mathbf{u}} \left[-\frac{\int_{\Omega} \tilde{\mathbf{e}}(\mathbf{u}) : \mathbf{C} : \tilde{\mathbf{e}}(\mathbf{u}) \, dV}{\int_{\Omega} \tilde{\boldsymbol{\sigma}}^{0} : \tilde{\mathbf{q}}(\mathbf{u}, \mathbf{u}) \, dV} \right]$$
(36)

To better illustrate the above aspects, we present a numerical study that isolates the effects of nonlocal interactions, modeled by the fractional-derivatives, on each of these stiffness terms of the nonlocal solid. This goal is achieved by conducting parametric studies designed to intentionally suppress the effect of nonlocal interactions either on the material or on the geometric stiffness term.

1. *Isolated Material Nonlocality*: For this case-study, the material stiffness matrix of the fractional-order structure (available from the weak model) is left unchanged. However, the geometric stiffness matrix is artificially modified to match its local elastic counterpart. More specifically, the fractional-order derivatives present within the expression of the geometric stiffness matrix are replaced by their integer-order counterparts. This formulation accounts for the effects of the nonlocal interactions only via the material stiffness matrix.

$$[K^b] = \int_0^L \frac{Eh^3}{12} [\tilde{B}_{\mathcal{H},11}]^T [\tilde{B}_{\mathcal{H},11}] \, \mathrm{d}x_1, \quad [G^b] = \int_0^L [B_{\mathcal{H},1}]^T [B_{\mathcal{H},1}] \, \mathrm{d}x_1 \tag{37a}$$

2. *Isolated Geometric Nonlocality*: In this case-study, the geometric stiffness of the fractional-order structure (available from the weak model) is unchanged, hence incorporating the effect of nonlocality. However, the fractional-order terms within the material stiffness are replaced by their integer-order counterpart. Therefore, the effect of nonlocality on the material stiffness is artificially suppressed. This case study allows focusing on the effect of nonlocality via the geometric stiffness matrix.

$$[K^b] = \int_0^L \frac{Eh^3}{12} [B_{\mathcal{H},11}]^T [B_{\mathcal{H},11}] \, \mathrm{d}x_1, \quad [G^b] = \int_0^L [\tilde{B}_{\mathcal{H},1}]^T [\tilde{B}_{\mathcal{H},1}] \, \mathrm{d}x_1 \tag{37b}$$

Note that $[\tilde{B}_{\square}]$ are the nonlocal strain-displacement matrices employing fractional-order derivatives and derived using f-FEM in Appendix A.2, and the matrices $[B_{\square}]$ are their local elastic analogue evaluated using integer-order derivatives as shown in [53]. It is clear that the stiffness terms evaluated using integer-order matrices corresponds to local elasticity. For the case of isolated material nonlocality with geometric stiffness terms being local, the softening effect introduced in $[K^b]$ by the fractional-order derivatives is expected to lead to lower values of critical load. In contrast, for the case of isolated geometric nonlocality with material stiffness terms being local, increasing the nonlocal effects would reduce the geometric stiffness, hence it will increase the critical load. These observations simply follow from the Rayleigh-Ritz expression in Eq. (13). In obtaining the above results we assumed a constant length scale throughout: $I_A = I_B = I_f$.

The results for the above described parametric studies are presented in Table 3 for the doubly clamped beam, and Table 4 for the simply-supported beam. For isolated material nonlocality ($[K^b]$: Nonlocal & $[G^b]$: Local), the critical load decreases monotonically as the degree of nonlocality increases, irrespective of the boundary condition. More specifically, the critical load is observed to decrease for reducing values of the fractional-order α and increasing values of the horizon of nonlocal influence l_f . Similarly, for isolated geometric nonlocality ($[K^b]$: Local & $[G^b]$: Nonlocal), the critical load is observed to increase with an increasing degree of nonlocality. It immediately follows that, when nonlocality is considered simultaneously in

Table 3
Critical loads for a double clamped (CC) beam. Results are non-dimensionalized following Eq. (35) and compared to study the effect of fractional theory constitutive parameters. Results are presented by artificially separating either the material or the geometric effects of nonlocality to track their individual effects on the critical load.

	Materia	l Nonlocal	ity		Geomet	Geometric Nonlocality			
α	1.0	0.9	0.8	0.7	1.0	0.9	0.8	0.7	
$l_f = 0.2L$	4.000	3.471	3.014	2.600	4.000	4.282	4.555	4.821	
$l_f = 0.4L$	4.000	2.912	2.124	1.551	4.000	4.893	5.930	7.130	
$l_f = 0.6L$	4.000	2.559	1.610	0.990	4.000	5.537	7.676	10.682	
$l_f = 0.8L$	4.000	2.411	1.421	0.810	4.000	5.986	9.068	13.999	
$l_f = L$	4.000	2.330	1.335	0.748	4.000	6.274	9.978	16.223	

Table 4
Critical loads for a simply-supported (SS) beam. Results are non-dimensionalized following Eq. (35) and compared to study the effect of fractional theory constitutive parameters. Results are presented by artificially separating either the material or the geometric effects of nonlocality to track their individual effects on the critical load.

	Materia	l Nonlocal	ity		Geometric Nonlocality			
α	1.0	0.9	0.8	0.7	1.0	0.9	0.8	0.7
$l_f = 0.2L$	1.000	0.978	0.958	0.939	1.000	1.095	1.183	1.263
$l_f = 0.4L$	1.000	0.937	0.877	0.815	1.000	1.220	1.464	1.735
$l_f = 0.6L$	1.000	0.887	0.776	0.653	1.000	1.362	1.841	2.481
$l_f = 0.8L$	1.000	0.840	0.689	0.536	1.000	1.482	2.201	3.304
$l_f = L$	1.000	0.803	0.630	0.469	1.000	1.568	2.478	3.986

both these stiffness terms, the critical load (Table 2) is the result of the *net* effect of these competing terms. This analysis explains the non-monotonic variation of the critical load with an increasing degree nonlocality.

Additional observations may be drawn from Table 2 following the parametric studies in Tables 3 and 4. It is clear from the table that non-locality increases the critical load for a SS beam while it decreases the critical load for a CC beam. We clarify that, while contrasting effects are noted for the two different boundary conditions, the effect of nonlocality on the system stiffness matrices is independent of the boundary conditions. Both the material stiffness [K] and the geometric stiffness [G] undergo a monotonic reduction with an increasing degree of nonlocality. This is established from the parametric studies in Tables 3 and 4. It is indeed the antagonistic effect between the reduction of the geometric and the material stiffness that determines the overall effect of the nonlocal interactions on the critical load. Therefore, the net effect of nonlocality may result in either higher or lower critical load for the structure depending on the relative reductions of the individual stiffness terms due to nonlocality. As observed in previous works using fractional-order approaches [32,33] and strain-driven integral approaches [13], the decrease in material stiffness of a SS beam, due to nonlocal elasticity, is less pronounced when compared to a CC beam. This suggests that the reduction in the material stiffness matrix [K^b] due to the fractional-order parameters (i.e. to the nonlocal effect) is offset, and subsequently dominated, by the simultaneous decrease in geometric stiffness matrix [G^b] (see Eq. (24)). This explains the higher critical load for a nonlocal SS beam compared to a local elastic beam. Contrarily, the softening effect on the material stiffness for the CC beam outweighs the simultaneous softening of the geometric stiffness, therefore resulting in marginally lower values of the critical load (compared to the local elastic beam).

Before proceeding further, we present the transverse mode shapes corresponding to the critical load of the beam and calculated by either integer-[1] or fractional-order approaches are compared in Fig. 4. While slight changes are noted in the curvature of buckling mode shapes for nonlocal beams, this effect is marginal even for very a pronounced degree of nonlocality, such as for $\alpha = 0.7$ and $l_f/L = 1$. These results highlight that the inclusion of the nonlocal effects via fractional-order modeling presents minimal effects on the buckling mode shape.

5.2. Plates

Consistently with the assumptions for the Kirchhoff plate theory, we selected a square plate with a=b and an aspect ratio a/h=100 to perform the current study. The 2D f-FEM model used in this section was developed and validated in [35]. Both a state of uniaxial compression $N_1=N_0$ and of biaxial compression $N_2=N_1=N_0$ were investigated. The critical loads were non-dimensionalized as follows [50]:

$$\overline{N}_0 = N_0 \times \frac{b^2}{\pi^2 D}, \quad D = \frac{Eh^3}{12(1 - v^2)}$$
 (38)

Accurate evaluation of the system matrices following 2D f-FEM requires the accurate evaluation of convolution integrals, along both the x_1 and x_2 directions. Thus, an appropriate choice for the dynamic rates of convergence is required in both directions. For this purpose, we define $\mathcal{N}_1^{inf} = l_f/l_{e_1}$ and $\mathcal{N}_2^{inf} = l_f/l_{e_2}$ where l_{e_1} and l_{e_2} are the discretized element dimensions of the uniform FE mesh along x_1 and x_2 directions, respectively. The convergence of the 2D discretized mesh used in this study is established for various choices of the fractional theory constitutive parameters in Table 5 for a simply supported (SSSS) plate subject to a uniaxial compressive load along the x_1 direction. Excellent convergence of the normalized critical loads is achieved, with differences of <1% between successive refinements of the mesh. Following this convergence study, we used $N_1^{inf} \times N_2^{inf} = 8 \times 8$ for the all the subsequent analyses.

As previously mentioned, the effect of the fractional-order nonlocality on the critical load was studied for two different cases of external loading: (1) uniaxial compression along x_1 ; (2) biaxial compression with equal loads applied along x_1 and x_2 . The critical loads for uniaxial (along x_1)

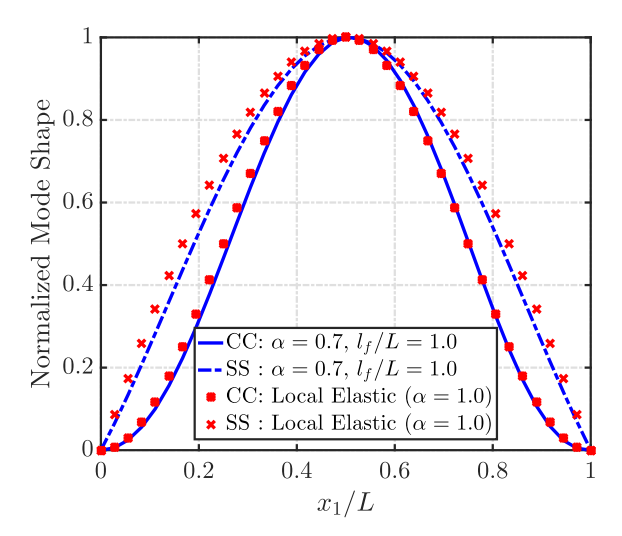


Fig. 4. Comparison of the buckling mode shapes obtained from either classical or fractional-order beam theory under different boundary conditions.

Table 5 2D f-FEM mesh convergence study. Non-dimensional critical load of a SSSS plate for different values of constitutive parameters α and l_f . In all cases, $N^{inf}=8$ guarantees a difference within 1% between successive refinements.

Fractional Horizon	infinf	fractional-order, α							
Length, l_f	$N_1^{inf} \times N_2^{inf}$	$\alpha = 1.0$	$\alpha = 0.9$	$\alpha = 0.8$	$\alpha = 0.7$				
$l_f = 0.5a$	4 × 4	4	4.120	4.183	4.178				
,	6×6	4	4.099	4.148	4.138				
	8×8	4	4.089	4.131	4.118				
	10×10	4	4.083	4.121	4.107				
$l_f = a$	4×4	4	4.258	4.445	4.545				
,	6×6	4	4.258	4.452	4.563				
	8 × 8	4	4.259	4.456	4.573				
	10×10	4	4.259	4.460	4.577				

Table 6
Critical loads for plate subject to uniaxial compression and various boundary conditions. Results are non-dimensionalized following Eq. (38) and compared to study the effect of the different fractional theory constitutive parameters. Recall that SSSS stands for simply supported; CCCC for fully clamped; and CFCF for plate clamped on two opposite edges and free on the other two.

	SSSS			CCCC				CFCF				
α	1.0	0.9	0.8	0.7	1.0	0.9	0.8	0.7	1.0	0.9	0.8	0.7
$l_f = 0.4a$	4	4.109	4.190	4.233	10.076	9.874	9.637	9.334	3.920	3.717	3.504	3.265
$l_f = 0.6a$	4	4.146	4.234	4.247	10.076	9.834	9.544	9.162	3.920	3.731	3.531	3.307
$l_f = 0.8a$	4	4.238	4.417	4.517	10.076	10.017	10.005	10.023	3.920	3.815	3.728	3.650
$l_f = a$	4	4.259	4.456	4.573	10.076	9.981	9.950	9.965	3.920	3.816	3.741	3.684

compression of plates, evaluated for selected values of α and l_f , are available in the Table 6. Additionally, the critical buckling loads for biaxial compression of plates are provided in Table 7. The tabulated results correspond to the following sets of boundary conditions [50]:

Simply supported (SSSS):
$$\begin{cases} x_1 = 0, a: & w_0 = \frac{\partial w_0}{\partial x_2} = 0 \\ x_2 = 0, b: & w_0 = \frac{\partial w_0}{\partial x_1} = 0 \end{cases}$$
 Clamped (CCCC):
$$\begin{cases} x_1 = 0, a: & w_0 = \frac{\partial w_0}{\partial x_1} = \frac{\partial w_0}{\partial x_2} = 0 \\ x_2 = 0, b: & w_0 = \frac{\partial w_0}{\partial x_1} = \frac{\partial w_0}{\partial x_2} = 0 \end{cases}$$
 Clamped-Free (CFCF):
$$x_1 = 0, a: w_0 = \frac{\partial w_0}{\partial x_1} = \frac{\partial w_0}{\partial x_2} = 0$$

where w_0 is the generalized displacement coordinate introduced in Eq. (25).

As evident from the Tables 6 and 7, the critical loads of fractional-order plates show a non-monotonic variation with increasing degree of nonlocality. While this observation deviates from the conclusions of studies based on classical integer-order nonlocal theories, it does agree with the results reported in §5.1 for nonlocal beams. Similar to the discussion in §5.1, this difference is a direct result of the simultaneous effect of the nonlocal response on both the geometric and material stiffness of the fractional-order plate. The increasing degree of nonlocality results in a

Table 7
Critical loads for plate subject to biaxial compression and various boundary conditions.
Results are non-dimensionalized following Eq. (38) and compared to study the effect of the different fractional theory constitutive parameters. Recall that SSSS stands for simply supported and CCCC for fully clamped.

	SSSS				CCCC			
α	1.0	0.9	0.8	0.7	1.0	0.9	0.8	0.7
$l_f = 0.4a$	2	2.055	2.098	2.125	5.304	5.112	4.917	4.706
$l_f = 0.6a$	2	2.074	2.120	2.136	5.304	5.086	4.862	4.613
$l_f = 0.8a$	2	2.119	2.210	2.266	5.304	5.212	5.146	5.099
$l_f = a$	2	2.129	2.230	2.293	5.304	5.196	5.123	5.075

Table 8

Critical loads for a fully clamped (CCCC) plate subject to biaxial compression. Results are non-dimensionalized following Eq. (38) and compared to study the effect of the different fractional theory constitutive parameters. Results are presented by artificially separating either the material or the geometric effects of nonlocality to track their individual effects on the critical load.

	Geometric Nonlocality							
α	1.0	0.9	0.8	0.7	1.0	0.9	0.8	0.7
$l_f = 0.4a$	5.304	3.763	2.650	1.845	5.304	6.880	8.909	11.538
$l_f = 0.6a$	5.304	3.437	2.197	1.378	5.304	7.583	10.901	15.832
$l_f = 0.8a$	5.304	3.265	1.987	1.188	5.304	8.098	12.496	19.635
$l_f^{'} = a$	5.304	3.123	1.817	1.039	5.304	8.467	13.663	22.448

Table 9

Critical loads for a simply-supported (SSSS) plate subject to biaxial compression. Results are non-dimensionalized following Eq. (38) and compared to study the effect of the different fractional theory constitutive parameters. Results are presented by artificially separating either the material or the geometric effects of nonlocality to track their individual effects on the critical load.

	Material	Nonlocalit	у		Geometric Nonlocality			
α	1.0	0.9	0.8	0.7	1.0	0.9	0.8	0.7
$l_f = 0.4a$	2.000	1.732	1.512	1.310	2.000	2.561	3.246	4.089
$l_f = 0.6a$	2.000	1.593	1.274	0.999	2.000	2.826	3.981	5.618
$l_f = 0.8a$	2.000	1.496	1.119	0.821	2.000	3.055	4.694	7.317
$l_f = a$	2.000	1.430	1.024	0.718	2.000	3.195	5.132	8.365

consistent reduction of the system stiffness matrices $[K^p]$ and $[G^p]$ given in Eq. (34c). More specifically, either reducing the numerical values of the fractional-order α or increasing the size of the domain of nonlocal influence l_f results in reduced values of $[K^p]$ and $[G^p]$. In agreement with the Rayleigh-Ritz expression for critical load given in Eq. (13), the individual reductions in these stiffness terms have a competing effect on the critical load for buckling of the nonlocal structure. To better illustrate the contrasting effect of reductions in material and geometric stiffness terms over the critical load, we conduct parametric studies that intentionally suppress the effect of nonlocal interactions either on the material or on the geometric stiffness term, similar to that conducted for beams.

The results of these parametric studies for buckling due to biaxial compression of the plates are provided in the Tables 8 and 9. More specifically, the critical loads for biaxial compression of a fully clamped plate, evaluated for the individual cases of isolated material and geometric nonlocality, are provided in Table 8. Similar studies were repeated for a plate subject to simply-supported boundary conditions and results are listed in Table 9. In both cases mentioned above, an increasing degree of nonlocality determines a monotonic reduction of the system stiffness (both material and geometric). However, as also noted previously in the case of beams, reducing the material and the geometric stiffness terms have an antagonistic effect on the critical load. In the case of isolated material nonlocality (i.e. reduced material stiffness; constant geometric stiffness), the critical load monotonically reduces with an increasing degree of nonlocality. In contrast, for the case of isolated geometric nonlocality (i.e. reducing geometric stiffness; constant material stiffness), the critical load monotonically increases with an increasing degree of nonlocality. Particularly interesting is the parallel between the case of isolated material nonlocality and classical (integer-order/strain-driven) models of nonlocal elasticity. Both these cases modify only the material stiffness that undergoes a reduction following an increasing degree of nonlocality. Thus, we observe a decreasing critical load which agrees with similar observations drawn following classical models in the literature [12,13]. We will discuss this aspect in detail in §5.3

Further, we note from Table 6 that the critical load for the nonlocal CCCC plate is lower than its local elastic analogue, while for the nonlocal SSSS plate the critical load is higher compared to the local elastic case. These contrasting observations can be explained by considering the pronounced influence of nonlocal effects on decreasing the material stiffness for plates subject to stiffer boundary conditions [35,36]. More specifically, a stronger reduction is noted in the material stiffness of fully clamped (CCCC) plate when compared to the simply supported (SSSS) plate. As discussed previously in the case of fractional-order SS beams, the weak reduction in material stiffness for SSSS plates is further dominated by the simultaneous decrease in geometric stiffness. Thus, the net result of nonlocal interactions on material and geometric stiffness terms is an increase in the critical load for SSSS plates. In contrast to this, the marked decrease in material stiffness for the clamped plate ensures lower critical load for CCCC fractional-order plates.

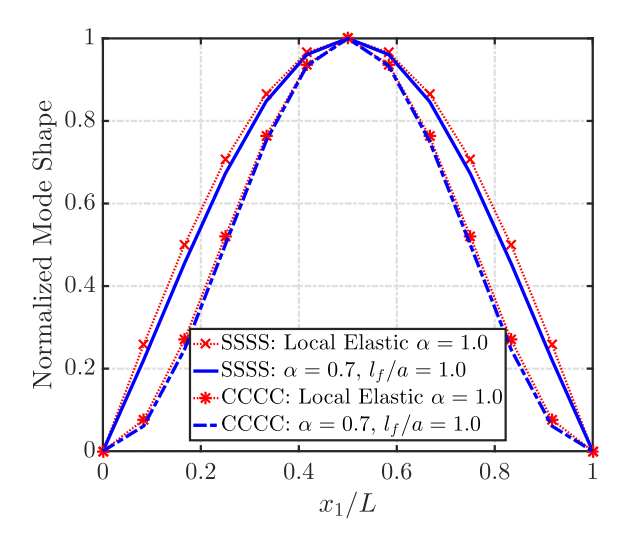


Fig. 5. Buckling mode shapes for biaxial compression obtained from either classical or fractional-order plate theory under different boundary conditions.

Finally, we compare the transverse mode shape along the length (x_1) at $x_2 = b/2$ corresponding to the critical load of the beams modeled via both integer-order [1] and fractional-order approaches. This comparison is illustrated in Fig. 5. In this figure, the effects of the nonlocal interactions are noted to be marginal on the mode shape of plate corresponding to critical buckling load. This observation is clearly in agreement with the previous study over fractional-order beams in Fig. 4. This is substantiated by the weak changes in curvature of the normalized modes for critical buckling of the nonlocal plate when compared with local analogues even for a case with high degree of nonlocality ($\alpha = 0.7$ and $l_f/a = 1.0$).

5.3. Comparison with existing integer-order nonlocal theories

In this section, we compare the effects of the nonlocal interactions on the critical load when accounted for by either fractional-order or integerorder theories of nonlocal elasticity.

Eringen's integral theory of nonlocal elasticity: We begin with a comparison of the critical load evaluated following fractional-order theory with that from the integer-order two-phase (i.e. local/nonlocal) model proposed in [54]. The latter choice is motivated by several studies in the literature that are based on this theory [21] or on simplified models derived from it [12,13,24,55] to study nonlocal effects on the critical load. The nonlocal constitutive relations take the following form of a Fredholm equation of the second kind [20]:

$$\tilde{\sigma}(\mathbf{X}) = \int_{\Omega} \overline{\mathcal{A}}_{e}(\mathbf{X}, \boldsymbol{\xi}) \, \mathbf{C} : \epsilon(\boldsymbol{\xi}) \, \mathrm{d}\boldsymbol{\xi}, \quad \overline{\mathcal{A}}_{e} = \chi_{1} \delta(\mathbf{X}, \boldsymbol{\xi}) + \chi_{2} \mathcal{A}_{e}(\mathbf{X}, \boldsymbol{\xi})$$

$$\tag{40}$$

where ϵ is the local strain evaluated using the classical integer-order strain-displacement relations. Also, $\delta(X, \xi)$ is the Dirac-delta defined at X, $\overline{\mathcal{A}}_e(X, \xi)$ and $\mathcal{A}_e(X, \xi)$ are the attenuation functions, χ_1 and χ_2 are positive material constants that satisfy: $\chi_1 + \chi_2 = 1$. Eringen's integral nonlocal model, corresponding to a Fredholm equation of the first kind, can be obtained for appropriate choices of χ_1 and χ_2 [20]. A detailed discussion on the comparison of the constitutive laws for the fractional-order and integer-order models of *linear* nonlocal elasticity is provided in [32]. In [32], the linear fractional-order continuum theory was obtained from the integral Eringen model assuming suitable choices of the attenuation function and the domain of influence. However, this equivalence holds only for the linear kinematic relations. For the geometrically nonlinear models of nonlocal elasticity, the constitutive models that follow the fractional-order kinematic relations in Eq. (1) cannot be deduced from Eringen's model in an analogous manner. This observation is relevant to understand the differences in critical load observed when using the fractional-order and the classical integer-order theories of nonlocal elasticity [12,13,21,24].

To elaborate further, we focus on the case of the nonlocal Euler-Bernoulli beam. The weak statement for the transverse equilibrium equation for the fractional-order nonlocal beam, that follows from Eq. (22), is given by:

$$\int_{0}^{L} \delta \{\Delta^{b}\}^{T} ([K^{b}] - N_{0}[G^{b}]) \{\Delta^{b}\} dx_{1} = \{0\}$$
(41)

where

$$[K^b] = \int_0^L \frac{Eh^3}{12} \left(D_{x_1}^{\alpha} w_0(x_1) \right)^2 dx_1, \quad [G^b] = \int_0^L \left(D_{x_1}^{\alpha} w_0(x_1) \right)^2 dx_1 \tag{42}$$

 $[K^b]$ and $[G^b]$ are the material and geometric stiffness matrices. Similarly, the expressions for these matrices derived following the integer-order nonlocal constitutive relations given in Eq. (40) would be [13,24]:

$$[K^b] = \int_0^L \int_0^L \frac{Eh^3}{12} \overline{\mathcal{A}}(x_1, x_1') \left(D_{x_1}^2 w_0(x_1) \right) \left(D_{x_1}^2 w_0(x_1') \right) dx_1 dx_1', \quad [G^b] = \int_0^L \left(D_{x_1}^1 w_0 \right)^2 dx_1$$

$$\tag{43}$$

Appropriate choices for the material constants χ_1 and χ_2 can reduce this model to the single-phase Eringen's model [12]. For the sake of comparison, we also provide below the expressions for the stiffness matrices evaluated assuming local elasticity [56]:

$$[K^b] = \int_0^L \frac{Eh^3}{12} \left(D_{x_1}^2 w_0(x_1) \right)^2 dx_1, \quad [G^b] = \int_0^L \left(D_{x_1}^1 w_0 \right)^2 dx_1 \tag{44}$$

Table 10

Non-dimensionalized critical load for Euler-Bernoulli nonlocal beam subject to different boundary conditions following Eringen's integral theory of nonlocal elasticity. Following [55], we choose $L=10\mathrm{nm}$ and h=L/100 (remaining parameters are retained from current study). Note the excellent agreement between the results from literature [55] and f-FEM modified in terms of the exponential kernel employed in [55].

	SS		CF		
κ (in nm)	Current	[55]	Current	[55]	
0 (Local)	9.8696	9.8696	2.4670	2.4670	
0.05	9.8671	9.8672	2.4472	2.4428	
0.5	9.6329	9.6319	2.2308	2.2259	
1	8.9864	8.9830	2.0050	2.0008	
2	7.0828	7.0761	1.6178	1.6156	

From Eq. (42), we note that fractional derivatives are present in the expressions for both the material and geometric stiffness matrices in the fractional-order theory. It is clear that these fractional derivatives capture the nonlocal interactions across the domain. The numerical values of these fractional derivatives, and thereby the stiffness terms, reduce following an increase in the degree of nonlocality. More specifically, reducing the fractional-order α and increasing the length scale l_f results in an increase in the softening influence of nonlocal interactions. This softening effect is evident from the results of the parametric studies in Tables 3, 4, 8 and 9. In the case of Eringen's integral models, the stiffness matrix $[K^b]$ in Eq. (43) includes nonlocal interactions across the domain and undergoes reduction with increasing degree of nonlocality. However, the geometric stiffness $[G^b]$ in this equation is unchanged by nonlocal interactions, and remains identical to its local form in Eq. (44). This observation is also noted in [12]. The decreasing values of stiffness $[K^b]$ with increasing degree of nonlocality, while $[G^b]$ remains constant, explains the lower critical load for nonlocal solids predicted by Eringen's theory [12,21]. This observation is akin to our parametric studies on fractional-order beams and plates over isolated material nonlocality (see Eq. (37a)).

We provide some numerical results to better illustrate the fact that the Eringen's integral nonlocal theory is similar to the case of isolated material nonlocality. This observation also supports the validation of the numerical method. We compare the critical loads for the nonlocal beam based on the commonly employed exponential attenuation kernel [55]. The constitutive relations for the integral theory of nonlocal elasticity are given in Eq. (40), where we consider $\chi_1 = 0$; $\chi_2 = 1$ and [55]:

$$\mathcal{A}_{e}(x_1, s_1, \kappa) = \frac{1}{2\kappa} \exp\left(-\frac{|x_1 - s_1|}{\kappa}\right) \tag{45}$$

is the exponential attenuation function, where κ is a material constant with dimensions of length. We evaluate the critical loads from the fractional finite element model for isolated material nonlocality. Details regarding the application of f-FEM to Eringen's theory can be found in our previous work [32]. The numerical results are non-dimensionalized following the relations given in Eq. (35). A comparison of the non-dimensionalized critical loads for SS and CF beams with results available in the literature is provided in Table 10. The difference between the present results and those presented in [55] is $\ll 1\%$, hence serving as validation of the numerical approach employed in this study. Note the monotonic reduction in critical loads with an increasing κ , which denotes an increase in the degree of nonlocality. This observation is to be expected, and further highlights the similarity between Eringen's theory and the case-study on isolated material nonlocality.

Finally, we also compare the fractional-order model with the Eringen's differential model of nonlocal elasticity. Continuing with the example of a Euler-Bernoulli beam, the corresponding nonlocal stiffness terms evaluated using the differential model of nonlocal elasticity are [57]:

$$[K^b] = \int_0^L \frac{Eh^3}{12} \left(D_{x_1}^2 w_0(x_1) \right)^2 dx_1, \quad [G^b] = \int_0^L \left[l_e^2 \left(D_{x_1}^2 w_0(x_1) \right)^2 + \left(D_{x_1}^1 w_0 \right)^2 \right] dx_1 \tag{46}$$

where l_e is the characteristic length scale [14]. Comparing the above expressions with Eq. (44), we note that the differential model predicts a modification in the geometric stiffness caused by the nonlocal interactions. However, the material stiffness is unchanged. More specifically, the material stiffness evaluated following the Eringen's differential model of nonlocal elasticity is identical to the classical local elasticity case given in Eq. (44). Therefore, the nonlocal effects on the critical load are realized only by a modification of the geometric stiffness matrix. This is unlike the previous observation of the effect of nonlocal elasticity being realized on both the stiffness matrices following fractional-order continuum theories (see Eq. (42)). From Eq. (46), we note increasing values of stiffness [G^b] with increasing degree of nonlocality, while [K^b] remains constant. This explains the lower critical load for nonlocal solids predicted by Eringen's differential models [15,24].

6. Conclusions

This work extends the fractional-order continuum framework to perform stability analysis of nonlocal solids. Thanks to the thermodynamically consistent and positive-definite form of the deformation energy density afforded by the fractional-order formulation, we can apply energy methods to perform the stability analysis. We reiterate that the geometrically nonlinear models of nonlocal elasticity, available within the framework of fractional calculus, allow the stability analysis to be conducted for nonlocal solids. As part of this approach, a general stability analysis is carried out for fractional-order solids by employing the Lagrange-Dirichlet theorem. The resulting approach allows studying scale effects, nonlocality, and heterogeneity on the stability of complex solids and interfaces. By specializing the approach to the case of linear buckling, we derive the critical load of nonlocal solids following Rayleigh-Ritz formalism. Our results show the capability of fractional-order models to account for the nonlocal effects on the material and geometric stiffness terms. This is unlike the classical integer-order models of nonlocal elasticity, where the nonlocal effects are restricted to only one of the stiffness terms. Thus, a more accurate account of the effects of nonlocal interactions on the stability of structures is realized by using the current fractional-order theory. In order to illustrate this observation in a more quantitative manner, the stability analysis was performed for fractional-order beams and plates, and the resulting eigenvalue problems were solved.

Declaration of Competing Interest

The authors declare that they have no known competing financial interests or personal relationships that could have appeared to influence the work reported in this paper.

CRediT authorship contribution statement

Sai Sidhardh: Conceptualization, Methodology, Software, Formal analysis, Writing - original draft, Visualization. Sansit Patnaik: Conceptualization, Methodology, Software, Formal analysis, Writing - original draft, Visualization. Fabio Semperlotti: Conceptualization, Methodology, Formal analysis, Writing - original draft, Writing - review & editing, Visualization, Supervision, Project administration, Funding acquisition.

Acknowledgements

The following work was supported by the Defense Advanced Research Project Agency (DARPA) under the grant #D19AP00052, and the National Science Foundation (NSF) under the grants #1761423 and #1825837. The content and information presented in this manuscript do not necessarily reflect the position or the policy of the government. The material is approved for public release; distribution is unlimited.

Appendix. A

A1. Linearization of the nonlinear fractional-order governing equations

This section details the derivation of the linearized fractional-order governing equations of equilibrium employed here. More specifically, the linearized governing equations in Eq. (21) for the Euler-Bernoulli beams will be derived from the nonlinear governing equations given in Eq. (17). This discussion is limited to the fractional-order Euler-Bernoulli beams for the sake of brevity. However, it may be extended with relative ease to Kirchhoff plates (Eq. (31)).

We consider two adjacent elastic states in equilibrium: (i) before the critical point; and (ii) at the onset of buckling. Now, the field distributions in Eq. (17) may be expressed as: 1) an initial component corresponding to response before the onset of the buckling, denoted by superscript \Box^i ; and 2) an additional component caused by the buckling, denoted by \Box^b . Note that, the response at the elastic state (i), before the onset of buckling, may be considered to be geometrically linear [58]. Following this, we express the stress resultants for the elastic state (ii) as:

$$N_{11} = N_{11}^i + N_{11}^b, \quad M_{11} = M_{11}^i + M_{11}^b \tag{46}$$

where N_{11}^i and M_{11}^i are the axial and bending stress resultants corresponding to elastic response before the onset of buckling, and N_{11}^b and M_{11}^b , respectively, correspond to the additional components generated by buckling. Assuming the beam remains straight (no initial curvature) before buckling ($w_0^i = 0$), we may write the transverse displacement caused by the buckling response to be $w_0 = w_0^b$. Here, distributed body forces F_k (k = 1, 2, 3) being absent, we employ the above definitions to linearize the nonlinear governing equations given in Eq. (17). At the onset of buckling, but before the critical point (elastic state (i)), we have:

$$w_0 = 0, \quad N_{11} = N_{11}^i, \quad M_{11} = M_{11}^i$$
 (47)

Substituting the above expressions into the nonlinear equations in Eq. (17) gives the governing equations for the elastic state at (i) as follows:

$$\mathfrak{D}_{x}^{a} N_{11}^{i} = 0 \ \forall x_{1} \in (0, L)$$
 (48a)

$$D_{x_1}^1 \left[\mathfrak{D}_{x_1}^{\alpha} M_{11}^i \right] = 0 \ \, \forall \, x_1 \in (0, L) \tag{48b}$$

These equations agree with results for linear elastic response of Euler-Bernoulli beams [32]. Subsequently, at the onset of buckling, the above derived linear governing equations are no longer applicable. Assuming small deformations at the onset of buckling $w_0^b \neq 0$, we substitute Eq. (46) into the nonlinear equations in Eq. (17). Following some mathematical operations employing the results from Eq. (48) for the adjacent elastic state (i),

$$\mathfrak{D}_{x_1}^{\alpha} N_{11}^b = 0 \ \forall \ x_1 \in (0, L)$$

$$D_{x_1}^1 \left[\mathfrak{D}_{x_1}^{\alpha} M_{11}^b \right] + N_{11}^i \mathfrak{D}_{x_1}^{\alpha} D_{x_1}^{\alpha} [w^b] = 0 \ \ \forall \ x_1 \in (0, L)$$
 (49b)

which are governing equations corresponding to the elastic state (ii). Note that the above expressions are identical to the linearized governing equations given in Eq. (21).

A2. Fractional finite element model

The finite element model developed above for the fractional-order model of nonlocal elasticity employs the fractional-order strain displacement matrices $[\tilde{B}_{\square}]$. These matrices are developed based on the RC fractional derivative given in Eq. (2) applied to the 1D and 2D Hermitian interpolation functions. As an example, we provide brief details for the numerical approximation of the 2D fractional derivatives $D_{x_1}^a[dw_0(x_1,x_2)/dx_2]$ and $D_{x_2}^a[dw_0(x_1,x_2)/dx_1]$ in this section; a complete account of the method can be found in [32,35]. Finite element approximations for all the 1D and 2D fractional derivatives can be obtained by following this procedure. From the definition given in Eq. (2), the above mentioned fractional derivatives can be written as:

$$D_{x_{1}}^{\alpha} \left[\frac{\partial w_{0}(x_{1}, y_{1})}{\partial x_{2}} \right] = \frac{1}{2} (1 - \alpha) \left[l_{A_{1}}^{\alpha - 1} \int_{x_{1} - l_{A_{1}}}^{x_{1}} \frac{D_{r}^{1} \left[\frac{\partial w_{0}(r, x_{2})}{\partial x_{2}} \right]}{(x_{1} - r)^{\alpha}} dr + l_{B_{1}}^{\alpha - 1} \int_{x_{1}}^{x_{1} + l_{B_{1}}} \frac{D_{r}^{1} \left[\frac{\partial w_{0}(r, x_{2})}{\partial x_{2}} \right]}{(r - x_{1})^{\alpha}} dr \right]$$
(50a)

$$D_{x_2}^{\alpha} \left[\frac{\partial w_0(x_1, y_1)}{\partial x_1} \right] = \frac{1}{2} (1 - \alpha) \left[l_{A_2}^{\alpha - 1} \int_{x_2 - l_{A_2}}^{x_2} \frac{D_s^1 \left[\frac{\partial w_0(x_1, s)}{\partial x_1} \right]}{(x_2 - s)^{\alpha}} \, ds + l_{B_2}^{\alpha - 1} \int_{x_2}^{x_2 + l_{B_2}} \frac{D_s^1 \left[\frac{\partial w_0(x_1, s)}{\partial x_1} \right]}{(s - x_2)^{\alpha}} \, ds \right]$$
(50b)

where r and s are dummy variables in the x_1 and x_2 directions, respectively. The above expressions can be recast as:

$$D_{x_{1}}^{\alpha} \left[\frac{\partial w_{0}(x_{1}, x_{2})}{\partial x_{2}} \right] = \int_{x_{1} - l_{A_{1}}}^{x_{1} + l_{B_{1}}} \mathcal{A}_{1}(\mathbf{X}_{0}, \mathbf{X}_{d}, l_{A_{1}}, l_{B_{1}}, \alpha) D_{r}^{1} \left[\frac{\partial w_{0}(r, x_{2})}{\partial x_{2}} \right] dr$$
(51a)

$$D_{x_2}^{\alpha} \left[\frac{\partial w_0(x_1, x_2)}{\partial x_1} \right] = \int_{x_2 - l_{A_2}}^{x_2 + l_{B_2}} \mathcal{A}_2(\mathbf{X}_0, \mathbf{X}_d, l_{A_2}, l_{B_2}, \alpha) \ D_s^1 \left[\frac{\partial w_0(x_1, s)}{\partial x_1} \right] \, \mathrm{d}s \tag{51b}$$

where the kernel $A_{\square}(\mathbf{X}_0, \mathbf{X}_d, l_A, l_B, \alpha)$ ($\square = 1, 2$), seen earlier in Eq. (3), is the fractional-order (α) power-law function connecting the point of interest $\mathbf{X}_0(x_1, x_2)$ and a dummy point $\mathbf{X}_d(r, s)$ within its domain of influence. As discussed previously, this domain of influence for the fractional-order derivative is position-dependent. The nonlocal horizons along the x_1 - and x_2 -directions are given by ($x_1 - l_{A_1}(\mathbf{X}), x_1 + l_{B_1}(\mathbf{X})$) and ($x_2 - l_{A_2}(\mathbf{X}), x_2 + l_{B_2}(\mathbf{X})$), respectively. The above mathematical statement allows the fractional derivative to be interpreted as a convolution of integer-order derivatives (from classical elasticity models) using the power-law kernel over the domain of influence. Therefore, it may be stated that the fractional-order continuum theory serves as a nonlocal model with power-law attenuation over distance. It follows from Eq. (50) that:

$$\mathcal{A}_{1}(\mathbf{X}_{0}, \mathbf{X}_{d}, l_{A_{1}}, l_{B_{1}}, \alpha) = \begin{cases} \frac{1}{2} (1 - \alpha) l_{A_{1}}^{\alpha - 1} (x_{1} - r)^{-\alpha} & r \in (x_{1} - l_{A_{1}}, x_{1}) \\ \frac{1}{2} (1 - \alpha) l_{B_{1}}^{\alpha - 1} (r - x_{1})^{-\alpha} & r \in (x_{1}, x_{1} + l_{B_{1}}) \end{cases}$$

$$(52a)$$

$$\mathcal{A}_{2}(\mathbf{X}_{0},\mathbf{X}_{d},l_{A_{2}},l_{B_{2}},\alpha) = \begin{cases} \frac{1}{2}(1-\alpha)l_{A_{2}}^{\alpha-1}(x_{2}-s)^{-\alpha} & s \in (x_{2}-l_{A_{2}},x_{2}) \\ \frac{1}{2}(1-\alpha)l_{B_{1}}^{\alpha-1}(s-x_{2})^{-\alpha} & s \in (x_{2},x_{2}+l_{B_{2}}) \end{cases} \tag{52b}$$

The above kernels depend on the relative distance between $\mathbf{X}_0(x_1, x_2)$ at which the derivative is evaluated and the dummy point $\mathbf{X}_d(r, s)$ within the fractional domain of influence and along a given direction.

The integer-order derivatives $D_r^1[\partial w_0(r,x_2)/\partial x_2]$ and $D_s^1[\partial w_0(x_1,s)/\partial x_1]$ within the convolution for fractional-order derivatives are expressed following the finite element approximations for generalized displacement coordinates as:

$$D_{r}^{1}\left[\frac{\partial w_{0}(r,x_{2})}{\partial x_{2}}\right] = [B_{\mathcal{H},21}(r,x_{2})]\{\Delta_{e}^{p}(r,x_{2})\}, \quad D_{s}^{2}\left[\frac{\partial w_{0}(x_{1},s)}{\partial x_{1}}\right] = [B_{\mathcal{H},12}(x_{1},s)]\{\Delta_{e}^{p}(x_{1},s)\}$$
 (53a)

where $[B_{H,21}(r,x_2)]$ and $[B_{H,12}(x_1,s)]$ are the integer-order strain-displacement matrices defined analogously to classical elasticity [53]. These matrices are defined over the 2D Hermite shape functions as:

$$[B_{\mathcal{H},21}(r,x_2)] = \frac{\partial}{\partial r} \left(\frac{\partial [\mathcal{H}(r,x_2)]}{\partial x_2} \right), \quad [B_{\mathcal{H},12}(x_1,s)] = \frac{\partial}{\partial s} \left(\frac{\partial [\mathcal{H}(x_1,s)]}{\partial x_1} \right)$$
(53b)

Finally, substitution of the above results in Eq. (51) gives the convolution-based finite element approximations for fractional-order derivatives:

$$D_{x_1}^{\alpha} \left[\frac{\partial w_0(x_1, x_2)}{\partial x_2} \right] = \int_{x_1 - l_{A_1}}^{x_1 + l_{B_1}} \mathcal{A}_1(\mathbf{X}_0, \mathbf{X}_d, l_{A_1}, l_{B_1}, \alpha) [B_{\mathcal{H}, 21}(r, x_2)] \{\Delta_e^p(r, x_2)\} dr$$
(54a)

$$D_{x_2}^{\alpha} \left[\frac{\partial w_0(x_1, x_2)}{\partial x_1} \right] = \int_{x_2 - l_{A_2}}^{x_2 + l_{B_2}} A_2(\mathbf{X}_0, \mathbf{X}_d, l_{A_2}, l_{B_2}, \alpha) [B_{\mathcal{H}, 12}(x_1, s)] \{ \Delta_e^p(x_1, s) \} \mathrm{d}s$$
 (54b)

The nonlocal interactions, characterized by the fractional derivatives, must include the contribution of other elements within the domain of influence. This would require the contributions from specific points in this domain to be associated with the corresponding (discretized finite) element and thereby the nodes of this element. For this purpose, we assemble the fractional-order strain-displacement matrices $[\tilde{B}_{\square}]$ before evaluating the global stiffness matrix. Such an approach also requires the assembly of nodal vectors corresponding to each element using appropriate connectivity matrices. A detailed discussion on these connectivity matrices is available for beams [32] and plates [35]. The fractional derivatives in Eq. (50), rewritten in terms of the global vectors of nodal displacements, is as follows:

$$D_{x_1}^{\alpha} \left[\frac{\partial w_0(x_1, x_2)}{\partial x_2} \right] = [\tilde{B}_{\mathcal{H}, 21}(x_1, x_2)] \{\Delta^p\} \quad D_{x_2}^{\alpha} \left[\frac{\partial w_0(x_1, x_2)}{\partial x_1} \right] = [\tilde{B}_{\mathcal{H}, 12}(x_1, x_2)] \{\Delta^p\}$$
 (55a)

where

$$[\tilde{B}_{\mathcal{H},21}(x_1, x_2)] = \int_{x_1 - l_{A_1}}^{x_1 + l_{B_1}} \mathcal{A}_1(\mathbf{X}_0, \mathbf{X}_d, l_{A_1}, l_{B_1}, \alpha) [B_{\mathcal{H},21}(r, x_2)] [\tilde{C}(\mathbf{X}_0, \mathbf{X}_d)] dr$$
(55b)

$$[\tilde{B}_{\mathcal{H},12}(x_1, x_2)] = \int_{x_2 - l_{A_2}}^{x_2 + l_{B_2}} \mathcal{A}_2(\mathbf{X}_0, \mathbf{X}_d, l_{A_2}, l_{B_2}, \alpha) [B_{\mathcal{H},12}(x_1, s)] [\tilde{C}(\mathbf{X}_0, \mathbf{X}_d)] ds$$
(55c)

where $[\tilde{C}(\mathbf{X}_0, \mathbf{X}_d)]$ is the connectivity matrix for elements enclosing the points $\mathbf{X}(x_1, x_2)$ and $\mathbf{X}_d(r, s)$. This matrix is non-zero only if the point (r, s) is within the domain of influence for (x_1, x_2) . As mentioned previously, the above procedure for the chosen example may be extended to other derivatives of the 1D and 2D Hermitian interpolation functions.

The numerical procedure for the evaluation of these numerical matrices includes successive steps of numerical integration. The first step of the numerical integration is performed over each point within the domain of influence in order to evaluate the nonlocal strain-displacement matrices, as shown in Eq. (55). This result is then utilized to determine the stiffness matrices given in Eqs. (24) and (34) which involves a numerical integration to be carried over the entire solid. The complete description of the numerical integration procedure to evaluate the system matrices for the fractional-order nonlocal structure can be found in [32,35].

References

- [1] Timoshenko SP, Gere JM. Theory of elastic stability. Courier Corporation; 2009.
- [2] Bažant ZP, Cedolin L. Stability of structures: elastic, inelastic, fracture and damage theories. World Scientific: 2010.
- [3] Arash B, Wang Q. A review on the application of nonlocal elastic models in modeling of carbon nanotubes and graphenes. Comput Mater Sci 2012;51(1):303–13.
- [4] Behera L, Chakraverty S. Recent researches on nonlocal elasticity theory in the vibration of carbon nanotubes using beam models: a review. Arch Comput Methods Eng 2017;24(3):481–94.
- [5] Romanoff J, Karttunen AT, Varsta P, Remes H, Reinaldo Goncalves B. A review on non-classical continuum mechanics with applications in marine engineering. Mech Adv Mater Struct 2020:1–11.
- [6] Patnaik S, Semperlotti F. A generalized fractional-order elastodynamic theory for non-local attenuating media. Proceedings of the Royal Society A 2020:476(2238):20200200
- [7] Zhu H, Patnaik S, Walsh TF, Jared BH, Semperlotti F. Nonlocal elastic metasurfaces: enabling broadband wave control via intentional nonlocality. Proceedings of the National Academy of Sciences 2020.
- [8] Alotta G, Di Paola M, Pinnola FP, Zingales M. A fractional nonlocal approach to nonlinear blood flow in small-lumen arterial vessels. Meccanica 2020:1–16.
- [9] Kröner E. Elasticity theory of materials with long range cohesive forces. Int J Solids Struct 1967;3(5):731–42.
- [10] Eringen AC, Edelen DGB. On nonlocal elasticity. Int J Eng Sci 1972;10(3):233–48.
- [11] Di Paola M, Failla G, Pirrotta A, Sofi A, Zingales M. The mechanically based non-local elasticity: an overview of main results and future challenges. Philosophical Transactions of the Royal Society A: Mathematical, Physical and Engineering Sciences 2013;371(1993):20120433.
- [12] Tuna M, Kirca M. Bending, buckling and free vibration analysis of euler-bernoulli nanobeams using eringens nonlocal integral model via finite element method. Compos Struct 2017:179:269–84.
- [13] Taghizadeh M, Ovesy HR, Ghannadpour SAM. Beam buckling analysis by nonlocal integral elasticity finite element method. Int J Struct Stab Dyn 2016;16(06):1550015.
- [14] Eringen AC. On differential equations of nonlocal elasticity and solutions of screw dislocation and surface waves. J Appl Phys 1983;54(9):4703–10.
- [15] Pradhan SC, Murmu T. Small scale effect on the buckling of single-layered graphene sheets under biaxial compression via nonlocal continuum mechanics. Comput Mater Sci 2009;47(1):268–74.
- [16] Reddy JN. Nonlocal theories for bending, buckling and vibration of beams. Int J Eng Sci 2007;45(2–8):288–307.
- [17] Challamel N, Zhang Z, Wang CM, Reddy JN, Wang Q, Michelitsch T, Collet B. On nonconservativeness of eringens nonlocal elasticity in beam mechanics: correction from a discrete-based approach. Archive of Applied Mechanics 2014;84(9–11):1275–92.
- [18] Romano G, Barretta R. Stress-driven versus strain-driven nonlocal integral model for elastic nano-beams. Composites Part B: Engineering 2017;114:184–8.
- [19] Eringen AC. Linear theory of nonlocal elasticity and dispersion of plane waves. Int J Eng Sci 1972;10(5):425–35.
- [20] Polizzotto C. Nonlocal elasticity and related variational principles. Int J Solids Struct 2001;38(42-43):7359-80.
- [21] Zhu X, Wang Y, Dai H-H. Buckling analysis of euler-bernoulli beams using eringens two-phase nonlocal model. Int J Eng Sci 2017;116:130–40.
- [22] de Sciarra FM. Variational formulations and a consistent finite-element procedure for a class of nonlocal elastic continua. Int J Solids Struct 2008;45(14–15):4184–202.
- [23] Sidhardh S, Patnaik S, Semperlotti F. Thermodynamics of fractional-order nonlocal continua and its application to the thermoelastic response of beams. European Journal of Mechanics-A/Solids 2021;88:104238.
- [24] Norouzzadeh A, Ansari R, Rouhi H. Pre-buckling responses of timoshenko nanobeams based on the integral and differential models of nonlocal elasticity: an isogeometric approach. Appl Phys A 2017;123(5):330.
- [25] Carpinteri A, Cornetti P, Sapora A. Nonlocal elasticity: an approach based on fractional calculus. Meccanica 2014;49(11):2551–69.
- [26] Mainardi F. Fractional relaxation-oscillation and fractional diffusion-wave phenomena. Chaos, Solitons & Fractals 1996;7(9):1461–77.
- [27] Patnaik S, Semperlotti F. Application of variable-and distributed-order fractional operators to the dynamic analysis of nonlinear oscillators. Nonlinear Dyn 2020;100(1):561–80.

- [28] Alotta G, Di Paola M, Failla G, Pinnola FP. On the dynamics of non-local fractional viscoelastic beams under stochastic agencies. Composites Part B: Engineering 2018;137:102–10.
- [29] Patnaik S, Sidhardh S, Semperlotti F. Towards a unified approach to nonlocal elasticity via fractional-order mechanics. Int J Mech Sci 2021;189:105992.
- [30] Povstenko Y. Fractional heat conduction in an infinite medium with a spherical inclusion. Entropy 2013;15(10):4122–33.
- [31] Sumelka W. Thermoelasticity in the framework of the fractional continuum mechanics. J Therm Stresses 2014;37(6):678–706.
- [32] Patnaik S, Sidhardh S, Semperlotti F. A Ritz-based finite element method for a fractional-order boundary value problem of nonlocal elasticity. Int J Solids Struct 2020:202:398–417.
- [33] Sidhardh S, Patnaik S, Semperlotti F. Geometrically nonlinear response of a fractional-order nonlocal model of elasticity. International Journal of Nonlinear Mechanics 2020;125:103529.
- [34] Tarasov VE, Aifantis EC. On fractional and fractal formulations of gradient linear and nonlinear elasticity. Acta Mech 2019;230(6):2043–70.
- [35] Patnaik S, Sidhardh S, Semperlotti F. Fractional-order models for the static and dynamic analysis of nonlocal plates. Commun Nonlinear Sci Numer Simul 2021;95:105601.
- [36] Patnaik S, Sidhardh S, Semperlotti F. Geometrically nonlinear analysis of nonlocal plates using fractional calculus. Int J Mech Sci 2020;179:105710.
- [37] Eringen AC. Theory of nonlocal thermoelasticity. Int J Eng Sci 1974;12(12):1063-77.
- [38] Lim CW, Zhang G, Reddy JN. A higher-order nonlocal elasticity and strain gradient theory and its applications in wave propagation. J Mech Phys Solids 2015;78:298–313.
- [39] Batra RC. Misuse of eringen's nonlocal elasticity theory for functionally graded materials. Int J Eng Sci 2021;159:103425.
- [40] Challamel N, Wang CM. The small length scale effect for a non-local cantilever beam: a paradox solved. Nanotechnology 2008;19(34):345703.
- [41] Eringen AC. Microcontinuum field theories: I. foundations and solids. Springer Science & Business Media; 2012.
- [42] Forest S, Sab K. Stress gradient continuum theory. Mech Res Commun 2012;40:16–25.
- [43] Mindlin RD, Eshel NN. On first strain-gradient theories in linear elasticity. Int J Solids Struct 1968:4(1):109–24.
- [44] Sidhardh S, Ray MC. Exact solutions for elastic response in micro-and nano-beams considering strain gradient elasticity. Mathematics and Mechanics of Solids 2019;24(4):895–918.
- [45] Samko SG, Kilbas AA, Marichev OI. Fractional integrals and derivatives: theory and applications. CRC: 1993.
- [46] Drapaca CS, Sivaloganathan S. A fractional model of continuum mechanics. J Elast 2012;107(2):105–23.
- [47] Szajek K, Sumelka W, Blaszczyk T, Bekus K. On selected aspects of space-fractional continuum mechanics model approximation. Int J Mech Sci 2020;167:105287.
- [48] Drucker DC. On the postulate of stability of material in the mechanics of continua. Tech. Rep.. Brown Univ Providence RI; 1963.
- [49] Hill R. On uniqueness and stability in the theory of finite elastic strain. J Mech Phys Solids 1957;5(4):229–41.
- [50] Reddy JN. Theory and analysis of elastic plates and shells. CRC press; 2006.
- [51] Wardle BL. Solution to the incorrect benchmark shell-buckling problem. AIAA journal 2008;46(2):381–7.
- [52] Norouzzadeh A, Ansari R. Finite element analysis of nano-scale timoshenko beams using the integral model of nonlocal elasticity. Physica E 2017;88:194– 200
- [53] Reddy JN. An introduction to nonlinear finite element analysis: with applications to heat transfer, fluid mechanics, and solid mechanics. OUP Oxford; 2014.
- [54] Altan SB. Uniqueness of initial-boundary value problems in nonlocal elasticity. Int J Solids Struct 1989;25(11):1271–8.
- [55] Tuna M, Kirca M. Exact solution of Eringen's nonlocal integral model for vibration and buckling of euler-bernoulli beam. Int J Eng Sci 2016;107:54-67.
- [56] Reddy J.N.. An introduction to the finite element method. 1989.
- [57] Pradhan SC. Nonlocal finite element analysis and small scale effects of CNT's with timoshenko beam theory. Finite Elem Anal Des 2012;50:8–20.
- [58] Turvey GJ, Marshall IH. Buckling and postbuckling of composite plates. Springer Science & Business Media; 2012.